University of Nebraska Medical Center
DigitalCommons@UNMC

Theses & Dissertations | Graduate Studies

Summer 8-13-2021

Development of Macromolecular Prodrug of Sinomenine for the Treatment of Rheumatoid Arthritis

Roshni Mukundan
University of Nebraska Medical Center

Tell us how you used this information in this short survey.

Follow this and additional works at: https://digitalcommons.unmc.edu/etd

 Part of the Immunology and Infectious Disease Commons, and the Pharmaceutics and Drug Design Commons

Recommended Citation

Mukundan, Roshni, "Development of Macromolecular Prodrug of Sinomenine for the Treatment of Rheumatoid Arthritis" (2021). *Theses & Dissertations*. 564.
https://digitalcommons.unmc.edu/etd/564

This Thesis is brought to you for free and open access by the Graduate Studies at DigitalCommons@UNMC. It has been accepted for inclusion in Theses & Dissertations by an authorized administrator of DigitalCommons@UNMC. For more information, please contact digitalcommons@unmc.edu.

DEVELOPMENT OF MACROMOLECULAR PRODRUG OF SINOMENINE FOR THE TREATMENT OF RHEUMATOID ARTHRITIS

by

Roshni Mukundan

A THESIS

Presented to the Faculty of
the University of Nebraska Graduate college
in Partial Fulfillment of the Requirements
for the Degree of Master of Science

Pharmaceutical Sciences Graduate Program

Under the Supervision of Professor Dong Wang

University of Nebraska Medical Center
Omaha, Nebraska

August, 2021

Advisory Committee:

Dong Wang, Ph.D.
Geoffrey Thiele, Ph.D.
Joseph A. Vetro, Ph.D.

ACKNOWLEDGMENTS

I would like to express my deep and sincere gratitude to my mentor Dr. Dong Wang for giving me this opportunity and for providing invaluable guidance throughout my research. His morals, sincerity, and wisdom inspired me both professionally and personally. He has taught me the manner to conduct research and to efficiently present it. I would like to thank him for his unwavering support especially during last year's pandemic. I would like to acknowledge the other members of my advisory committee: Dr. Geoffrey Thiele and Dr. Joseph Vetro for their constant encouragement, insightful remark, and support in my research and career path.

My colleagues at Dr. Wang's lab were nothing short of a delight to work. They have guided and supported me in all possible ways during my research. Dr. Zhenshan Jia has been kind and welcoming since I joined the lab. He imparted his proficiency in chemistry and has been an immense help throughout my research. Dr. Xin Wei has shared her mastery in *in vivo* work and in designing of experiments. She has always been there whenever I needed any help and has provided me with various recommendations. I would like to extend my gratitude to Dr. Gang Zhao for his advice and guidance on various instrumentation. Ningrong Chen and Zhifeng Zhao invariably have been there whenever I required a helping hand and have given me valuable inputs during my research. Haochen Jiang has not only assisted with my experiments but has also been a great friend. She has shown a sympathetic ear to my struggles and has been supportive. I would also like to thank all the other members of my lab.

I would like to extend special thanks to Dr. Subodh Lele for graciously agreeing to help with the histological assessment and share his expertise in it. I would also like to

thank all the professors and instructors of the various courses during my graduate program and to all the staff at the Department of Pharmaceutical Sciences.

Lastly, I convey my sincere gratitude to my family and friends. I would like to especially thank my mother, brother, and sister-in-law for trusting and believing in me even when I did not. None of this would have been possible without their continuous love, support, and motivation. I am eternally indebted to them for the giving me this chance and experience that have made me who I am.

ABSTRACT

DEVELOPMENT OF MACROMOLECULAR PRODRUG OF SINOMENINE FOR THE TREATMENT OF RHEUMATOID ARTHRITIS

Roshni Mukundan, M.S.

University of Nebraska Medical Center, 2021

Advisor: Dong Wang, Ph.D.

Inflammation is a natural response of the body to infections or any potential threat to the body. But, sometimes the immune system attacks its own body causing persistent inflammation leading to inflammatory diseases. One of the common chronic inflammatory diseases is rheumatoid arthritis (RA) which causes inflammation of the synovial membrane. The current treatments for RA are effective in controlling the symptoms but they come with severe side effects and economic burden. Further, the management of pain is still a problem with these drugs. Sinomenine is a natural alkaloid obtained from the Chinese medicinal plant *Sinomenium acutum* that has been used to clinically treat RA for several years in China. They exhibit various pharmacological effects like anti-inflammatory, anti-arthritis, and analgesic effects etc. which makes it favorable in treating rheumatic diseases. Yet again, sinomenine has some disadvantages like poor bioavailability, short half-life, and systemic toxicity etc. Therefore, in this thesis we concentrated on developing a macromolecular prodrug of sinomenine and evaluated its therapeutic and analgesic efficacy in an animal model of monoarticular antigen induced arthritis (MAA). To address the current drawbacks of sinomenine, we developed this macromolecular prodrug as a thermoresponsive hydrogel and administered it to the animals by intra-articular injection. We showed that the HPMA copolymer sinomenine can

form hydrogel and can be retained in the knee joint for a span of twenty one days. The results from the pain evaluation tests also confirmed their potential to exhibit local analgesic effects without any potential toxicity. They also demonstrated the absence of spinal cord analgesia which helps prevent tolerance and addiction. We can conclude from these results that this macromolecular prodrug of sinomenine may have a potential for the management of pain in RA.

TABLE OF CONTENTS

LIST OF FIGURES

LIST OF TABLES

LIST OF ABBREVIATIONS

AIBN	2,2′- azobisisobutyronitrile
ALT	Alanine aminotransferase
ALB	Albumin
ALP	Alkaline phosphate
AMY	Amylase
ANOVA	One-way analysis of variance
APMA	N-(3-Aminopropyl) methacrylamide
BMD	Bone mineral density
BMI	Body mass index
BS/TV	Bone surface density
BV/TV	Percent bone volume
COX	Cyclooxygenase
CTA	Chain transfer agent
CRE	Creatinine
DMARDs	Disease-modifying anti-rheumatic drugs
DMSO	Dimethyl sulfoxide
DMEM	Dulbecco’s modified eagle medium
DMF	Dimethylformamide
ESR	Erythrocyte sedimentation rate

FLS	Fibroblast like synoviocytes
FPLC	Fast protein liquid chromatography
FDA	U.S Food & Drug Administration
FBS	Fetal bovine serum
gf	Gram force
GLOB	Globulin
HLA	Human leukocyte antigen
HCl	Hydrochloric acid
HPMA	*N*-(2-Hydroxypropyl) methacrylamide
HOAc	Acetic acid
HPLC	High performance liquid chromatography
H&E	Hematoxylin and eosin
IACUC	Institutional Animal Care and Use Committee
IL-1	Interleukin-1
IL-6	Interleukin-6
IA	Intra-articular
JAK	Janus kinase
K^+	Potassium
M_n	Number average molecular weight
M_w	Weight average molecular weight

MAA	Monoarticular antigen induced arthritis
MeOH	Methanol
MAOI	Monoamine oxidase inhibitor
mBSA	Methyl bovine serum albumin
MPE	Maximum possible effect
MMP-3	Matrix metalloproteinase-3
MRI	Magnetic resonance imaging
Na^+	Sodium
NaOH	Sodium hydroxide
NH_2NH_2	Hydrazine monohydrate
NRI	Norepinephrine reuptake inhibitor
NSAIDs	Nonsteroidal anti-inflammatory drugs
OA	Osteoarthritis
PAM	Pressure application measurement
PHOS	Phosphorous
PI	Pre-induction
P-Sino	ProGel Sinomenine
P-Sino L	ProGel Sinomenine low dose group
P-Sino H	ProGel Sinomenine high dose group
PT	Pre-treatment

RA	Rheumatoid arthritis
RBC	Red blood cells
RF	Rheumatoid factor
RAFT	Reversible fragmentation-addition chain transfer
SEC	Size exclusion chromatography
SNP	Single nucleotide polymorphisms
SNRI	Selective serotonin noradrenaline reuptake inhibitor
SSRI	Selective serotonin reuptake inhibitor
T_{gel}	Gelation temperature
Tb.N	Trabecular number
Tb.Sp	Trabecular separation
Tb.Th	Trabecular thickness
TCAs	Tricyclic antidepressants
TNF	Tumor necrosis factor
TCM	Traditional Chinese medicine
WBC	White blood cells
WBS	Weight bearing score
μOR	mu opioid receptor

LIST OF CONTRIBUTORS

1. Chapter 2- Dr. Zhenshan Jia designed and guided the synthesis of P-Sinomenine, P-Sino-IRDye-800CW , and P-Sino-Alexa flour 647. Zhifeng Zhao helped with preliminary *in vitro* hydrogel release study and Ningrong Chen guided the sol-gel phase transition diagram. Dr. Gang Zhao supervised the drug loading study.

2. Chapter 3- Dr. Xin Wei trained the pain evaluation tests performed on the animals. Ningrong Chen, Haochen Jiang, and Dr. Zhenshan Jia helped with the animal studies. Zhifeng Zhao helped in performing the safety and toxicity study. Ningrong Chen and Dr. Zhenshan Jia helped during euthanizing the animals. Ningrong Chen and Dr. Gang Zhao guided the micro-computed tomography analysis. Dr. Subodh M. Lele helped in the histological evaluation.

CHAPTER 1

INTRODUCTION

1.1Rheumatoid arthritis

Rheumatoid arthritis (RA) is an autoimmune disease affecting multiple joints symmetrically. It is a systemic chronic inflammatory disease affecting almost 1% of the population globally. Women are more inclined to the disease than men, and it commonly begins between the ages of 40-60 years [1, 2]. It is characterized by inflammation of the synovial membrane which, can result in swelling of the joints, pain, stiffness, and eventually to deformity and bone destruction. Over time if not treated properly can lead to disability [2, 3]. The presence of autoantibodies (rheumatoid factor and anti–citrullinated protein antibody etc.) leads to the infiltration of immune cells in the joints causing the above-mentioned symptoms. Aside from joints, RA may also affect the organs. This extra-articular manifestation usually appears in organs like; skin, lungs, heart, etc. The occurrence of these manifestations varies depending on the place, gender, and immune proteins [4]. RA can be diagnosed primarily based on physical examination (presence of at least one swollen joint), and blood and imaging tests (ultrasound and magnetic resonance imaging (MRI)). The progression of the disease can be slowed with early diagnosis and treatment [5, 6]. Nonsteroidal anti-inflammatory drugs (NSAIDs), glucocorticoids, disease-modifying anti-rheumatic drugs (DMARDs) and biologic DMARDs are the current treatment options for RA. The NSAIDs and corticosteroids are used as first-line therapy, alone or in combination, and when this therapy is ineffective, the second-line treatments (DMARDs) are promoted. During the end stage of the disease when all the nonsurgical options have failed

leading to persistent joint pain and immobility of the joint, surgery is used as the final resort [3, 7, 8].

1.2 Risk factors leading to development of RA

Both genetic and environmental factor increases the disposition for RA. The class II alleles of human leukocyte antigen (HLA) are linked with RA, especially the subtype HLA-DR4. These alleles (DRB1) have a shared epitope, that is, a similar amino acid sequence. Individuals who have these shared epitopes are susceptible for RA than others. Single nucleotide polymorphisms (SNPs) are a non-HLA gene that is also associated with the risk of developing RA. In addition to these there are other loci that has a role in the genetic susceptibility of the disease like the PTPN22 and IL23R genes [9, 10].

A major environmental factor that contributes to RA is smoking. Studies have shown the link between smoking with both the development of RA and an increase in the severity of disease. This is also supported by the high immune complexes (autoantibody like anti-citrullinated protein antibody (ACPA) etc.) present in those individuals. Furthermore, the existence of the HLA-DR shared epitope gene might provoke the reactions to citrullinated proteins showing the association between gene and environmental factors [11].

1.3 Current treatment in RA

The present treatment for RA includes various classes of drugs mainly focused on reducing the inflammation and pain, thereby preventing any deformity. The nonsteroidal anti-inflammatory drugs (NSAIDs) are widely used to alleviate the above-mentioned symptoms of RA. Their underlying mechanism in providing analgesia and reducing inflammation is by inhibiting the enzyme cyclooxygenase (COX). These NSAIDs can either non-specifically impede both COX-1 and COX-2 or selectively

impede COX-2. Even though they are effective in controlling the disease, they have some adverse effects like gastrointestinal, nephrotoxicity, and cardiovascular toxicity [12, 13].

Corticosteroids are a class of drugs that are used to treat conditions like inflammatory diseases, asthma, allergies, dermatitis etc. The mechanism of action of glucocorticoids is dependent up their diffusing through the cell membrane and interacting with the cytosolic GC receptor. This interaction leads to changes in the gene transcription causing transactivation or transrepression of the inflammatory genes. Corticosteroids are administered orally, or intra-articular injections are given to treat the local inflammation. Even though they are an essential part in a lot of inflammatory and immunologic diseases, they have posed severe risks like osteoporosis, adrenal suppression, cardiovascular disease etc. [7, 14].

Disease modifying anti-rheumatic drugs (DMARDs) are used to treat many inflammatory arthritis and some kinds of cancers. They are usually classified as traditional and biologic DMARDs and provide immunosuppressive and immunomodulatory effects. They help in improving the physical function and prevent further damage of the joints. Methotrexate, sulfasalazine, leflunomide, and hydroxychloroquine are the most frequently used traditional DMARD. Methotrexate is predominantly used as monotherapy or in combination with other drugs. They reduce the immune response by prohibiting the enzyme dihydrofolate reductase from converting dihydrofolic acid to folinic acid thereby inhibiting the propagation of immune cells. Ultimately, the process by which the DMARDs help in RA is by hampering the important pathways in the inflammatory cascade [15-17]. A more recent remedy in the management of RA are the biologic DMARDs. They provide a more targeted effect and are more efficacious in slowing down the progression of the disease. Yet again they bear the issue of having long term safety and serious side effect like infections

and lymphoma. Most of the biologic DMARDs are tumor necrosis factor alpha (TNF-α) inhibitors as TNF-α plays an important role in boosting the inflammation in the joint. The prevalent anti-TNF drugs are etanercept, infliximab, adalimumab etc. The other biologics available are anakinra, tocilizumab, etc. These act by either binding to the interleukin-1 (IL-1) or by blocking interleukin-6 (IL-6) which are vital messengers in the inflammation process. More recently approved small molecule inhibitors are upadacitinib and baricitinib, which are Janus Kinase (JAK) inhibitors. Unfortunately, biologics are very expensive and cause an economic burden to the patients. The overall burden is higher in cases of developing countries where there is a shortage of finance and health care services [7, 18, 19].

In spite of the current available medications for RA, the management of pain due to arthritis remains a top priority. Opioids are commonly prescribed at some point to control this pain. They act by the ubiquitous opioid receptors like the μOR (mu opioid receptor). This receptor is the fundamental objective for pain relief. The use of weak opioids like codeine, dextropropoxyphene, and tramadol are known to have beneficial analgesic effects when used for a short period of time. But the long-term use of these opioids draws the concern of safety and shows decreased efficacy. In addition, they also have the concern of opioid misuse [20, 21]. Antidepressants used in the treatment of RA augment pain relief, mood, sleep, and other functional status. The various types of antidepressants based on their conformation and mechanism are tricyclic antidepressants (TCAs), monoamine oxidase inhibitors (MAOIs), selective serotonin reuptake inhibitors (SSRIs), selective serotonin noradrenaline reuptake inhibitors (SNRIs) and norepinephrine reuptake inhibitors (NRIs). They both use the spinal and supraspinal mechanism of action by crossing the blood brain barrier but their exact mechanism in providing analgesic effect in RA is ambiguous and contentious [22, 23].

1.4 Challenges with current treatment

As mentioned previously, the various classes of drugs used in treating RA come with several side effects and economic burden. The variation in the effect of treatment could also arise due to the genetic profile, comorbidities, extra-articular manifestations, and environmental factors. In addition, the age and gender of the patients also plays a role in response to the treatment. But mainly these medications have poor bioavailability and short half-lives which compels frequent dosage [24].

With respect to the comorbidities, a high body mass index (BMI) can have a serious impact in the treatment outcome. This has been proven in the case of TNF inhibitors. The presence of very high titers of autoantibodies can be indicative of extra-articular manifestations and it is essential to treat these immediately [25].

Therefore, an effective targeted treatment is required for RA that would avoid untimely clearance of the drug and systemic toxicity. The recent advances in nanotechnology and novel drug delivery systems can help in abridging the gap present in the management of the disease.

1.5 Sinomenine

Sinomenine (7,8 -didehydro-4-hydroxy-3,7- dimethoxy-17-methylmorphinan-6-one), is a natural alkaloid which is obtained from the stem and roots of the Chinese herbal plant *Sinomenium acutum*. It is the primary active chemical component of this plant with various pharmacological effects. It is an established medicine in China and Japan where it is used to treat arthritic and rheumatic diseases. Zhengqing Fengtongning is a sinomenine hydrochloride tablet that is used to treat RA which is known to effectively reduce the indexes of erythrocyte sedimentation rate (ESR) and RF. Clinical studies show that sinomenine may mitigate the symptoms of RA and is more efficacious than NSAIDs [26]. There are also studies showing the effective

response of sinomenine in combination with methotrexate against RA [27]. The diverse pharmacological effects displayed by sinomenine are anti-inflammatory, immunosuppressive, analgesic, anti-arthritic effect etc. Sinomenine has an anti-proliferative effect on the fibroblast like synoviocytes (FLS) and inhibits the pro-inflammatory cytokines resulting in the preservation of the tissues in the joints. Additionally, sinomenine has a strong histamine releasing property [3, 28-31]. Apart from being effective against rheumatism they are also efficacious in treating pain against different types of neuralgia, osteoarthritis (OA), systemic lupus erythematosus etc.

The structure of sinomenine is similar to the other natural alkaloids like morphine. All of them share the phenanthropiperidine moiety. Sinomenine consists of three major functional groups namely trialkylamine, α,β-unsaturated ketone, and tetrasubstituted aromatic ring. They have a tetracyclic framework which is analogous to codeine and dextromethorphan [32]. An advantage of sinomenine over opioids like morphine is that they boost the threshold of pain without developing any tolerance. In addition, they do not show any central inhibitory effects which is present in the case of morphine [31].

Some studies were done to determine the physiochemical properties of sinomenine hydrochloride as it is beneficial while using in drug delivery systems. The pKa of sinomenine hydrochloride is around 7.98, log*P* of 1.34, molecular weight of 365 Da, and solubility in water is 118 mg/mL [33].

Studies performed to evaluate the pharmacokinetics of sinomenine showed that a peak concentration of the drug is reached within the first thirty minutes and even repeated administration of the drug did not result in the accretion of the drug showing its poor bioavailability [34]. Investigation was also done to determine the pharmacokinetics of sinomenine monomer and the extracts from the plant

Sinomenium acutum. This study showed that there was a difference in the pharmacokinetics between the sinomenine monomer and the extract with the latter showing a lower concentration in the blood [35]. Evidences show that the tissue distribution of sinomenine is mainly in kidneys and liver which are the main sites of metabolism and clearance. This shows that sinomenine's elimination is through the hepatobiliary system and may be managed by P-glycoprotein and the metabolism may be by P-450 [36]. The phase I metabolism of sinomenine leads to two metabolites namely demethyl-sinomenine and hydroxylated-sinomenine [37].

1.6 Limitations to the use of sinomenine

Though sinomenine is proven to have some beneficial effects against RA, it has a few drawbacks. They have a short half-life, low oral bioavailability, and the concentration of sinomenine in the blood is varying. Studies have also shown that the long-term oral administration of sinomenine hydrochloride causes gastrointestinal, liver, cardiovascular toxicity, and they also undergo the phenomena of first-pass effect. Apart from the oral administration, even the intramuscular injections pose some adverse effects like rashes due to the release of histamines. To overcome these limitations, different drug delivery systems were adopted such as transdermal drug delivery system, liposomes, polymeric nanocarriers, gels, microemulsions, etc. These help in preventing the systemic toxicity, produce sustained release, improve the bioavailability, and have a prolonged retention [30, 33, 38-42].

1.7 HPMA and injectable hydrogels

N-(2-hydroxypropyl)methacrylamide (HPMA) copolymers are water-soluble polymers that are widely used in drug delivery systems. The non-immunogenic and non-toxic properties of this copolymer has made it a promising carrier. It is shown that these macromolecules are taken up into the cells by endocytosis and finally into the

lysosomal compartment which help in releasing the drug. Typically, the drug is conjugated to the backbone or branches of this copolymer. Also, in vivo studies have demonstrated these polymers to be degradable[43]. Due to these advantages, HPMA are used in prodrugs and in hydrogels. This essentially helps in overcoming the drug toxicity, drug resistance, and improved drug targeting[44]. The HPMA conjugated doxorubicin was the first macromolecular prodrug to enter clinical trials[45]. In our laboratory, we have shown the preferred targeting, accumulation, and retention of HPMA based prodrugs and hydrogels in inflammatory models of arthritis[46-50].

Hydrogels are polymers that are made up by the cross-linking of hydrophilic polymers. They are available in different forms like nanoparticles, coating, films etc. which allows for its application in tissue engineering, regenerative medicine, and drug delivery. Among the various advantages of hydrogels, an important one is the ability to maintain high concentration of the drug at the desired site for long periods of time[51]. The physical form of hydrogels can undergo a change in its state from liquid to gel depending on the environmental stimuli like temperature, pH, ionic concentration etc.

In order to have a sustained release, improve the residence time, and bioavailability of the drug, various research groups have tried implementing the use of in situ gel systems. In addition, alternate mode of administering the drug like intra-articular (IA) injections have also been tested. Previously, studies were done in treating uveitis by using sinomenine hydrochloride in situ gels. Also, because of the rapid expulsion of sinomenine in vivo, intra-articular administration of the drug could be beneficial in improving the therapeutic efficacy [52-54].

In this thesis, we hypothesize that the newly designed HPMA copolymer conjugate of sinomenine in an injectable hydrogel form can improve the therapeutic and analgesic efficacy by intra-articular injection in a monoarticular antigen (MAA)

induced arthritis model. We believe that the chemically conjugated sinomenine to the HPMA by an acid labile hydrazone bond will be cleaved due to the low pH at the inflamed site. As mentioned above, the intra-articular injection of ProGel Sinomenine at the inflamed joint will improve its retention at the joint with sustained release.

CHAPTER 2

SYTHESIS AND CHARACTERIZATION OF PROGEL SINOMENINE

2.1 Introduction

As mentioned in the preceding chapter, sinomenine is natural alkaloid whose structure resembles to natural opioids like morphine. Clinically they are proven to be beneficial for RA, but they have certain limitations pertaining to their bioavailability, half-life, and concentration in the blood. Hence, better deliver systems are required to offset these limitations. Previously, our lab has developed macromolecular prodrugs of various drugs in treatment against inflammatory arthritis. They have shown promising results by selectively accumulating in the inflammatory sites and retained at the desired site during the course of the treatment. Also, they showed enhanced therapeutic effect compared to the parent drug and with limited systemic toxicity. Therefore, in this chapter we synthesized a macromolecular prodrug as a thermoresponsive hydrogel which can retain in the joint and produce a sustained release. It is a *N*-(2-Hydroxypropyl) methacrylamide (HPMA) copolymer based sinomenine prodrug which is synthesized by polymer analogous reaction. Further the synthesized copolymer is evaluated for its drug loading, drug release, and hydrogel forming capability.

2.2 Materials and Methods

2.2.1 Materials

N-(3-Aminopropyl) methacrylamide (APMA) hydrochloride was acquired from Oakwood chemical (Estill, South Carolina) and *N*-(2-Hydroxypropyl) methacrylamide (HPMA) was synthesized as previously reported [55]. CTA, Alexa flour 687, IRDye 800CW was purchased from LI-COR Biosciences (Lincoln, NE). APMA-Terephthalate-

OMe was prepared as reported in literature [48]. Sinomenine hydrochloride was procured from LKT laboratories Inc. (St Paul, Minnesota) (purity >98%).

2.2.2. Instruments

The weight average molecular weight (M_w) and the number average molecular weight (M_n) of the synthesized copolymer were found by size exclusion chromatography (SEC) using the ÄKTA FPLC system (GE Healthcare, Chicago, IL) equipped with UV and RI (Knauer, Berlin, Germany) detectors. The column used to perform the SEC was a Superdex peptide 10/300 GL column with 70% acetonitrile-phosphate buffered saline (pH 7.4) as the mobile phase. All the HPLC analysis were done using Agilent 1100 system (Agilent Technologies, Inc., Santa Clara, CA) with a C_{18} reverse phase column (Poroshell 120) with the column specification 4.6 x 250mm, 2.7 µm (Agilent). Thermo Scientific multi-blok heater was used for the sol-gel phase transition diagram.

2.2.3 Synthesis of ProGel Sinomenine

ProGel Sinomenine was synthesized by the mechanism of polymer analogous reaction. HPMA (1.2 g, 8.37 mmol), APMA-Terephlate-OMe (448 mg, 1.48 mmol), APMA hydrochloride (18.8 mg, 0.1 mmol), along with RAFT agent S,S′-bis (α, α′-dimethyl-α″-acetic acid)-trithiocarbonate (CTA) (58.2 mg, 0.21 mmol) and initiator 2,2′-azobisisobutyronitrile (AIBN) (60.9 mg, 0.37 mmol) were dissolved in methanol (12 mL). This solution was transferred to an ampule and purged with Argon for around a minute to protect from oxygen. The ampule was then sealed and kept in a heated oil bath for polymerization that was set at 55 °C and stirred for 48 hours. After the polymerization reaction, hydrazine monohydrate (1.5 g) was added, and the polymeric solution was stirred overnight. The solvent was removed using a rotary evaporator and the residue was purified by column chromatography (LH-20) to remove any unreacted

hydrazine. The obtained product was lyophilized to get the hydrazide polymer (1.40 g). To the resulting hydrazide containing HPMA copolymer (1.0 g), sinomenine (0.84 g, 2.63 mmol) and acetic acid (4 mg) was added and dissolved in a mixture of methanol (5 mL) and water (1 mL). This solution was then stirred again for 24 hours. After which the final polymeric solution was filtered, and the filtrate was purified using a LH-20 column to remove any unreacted small molecules. After lyophilization, 1.20 g of ProGel Sinomenine was obtained.

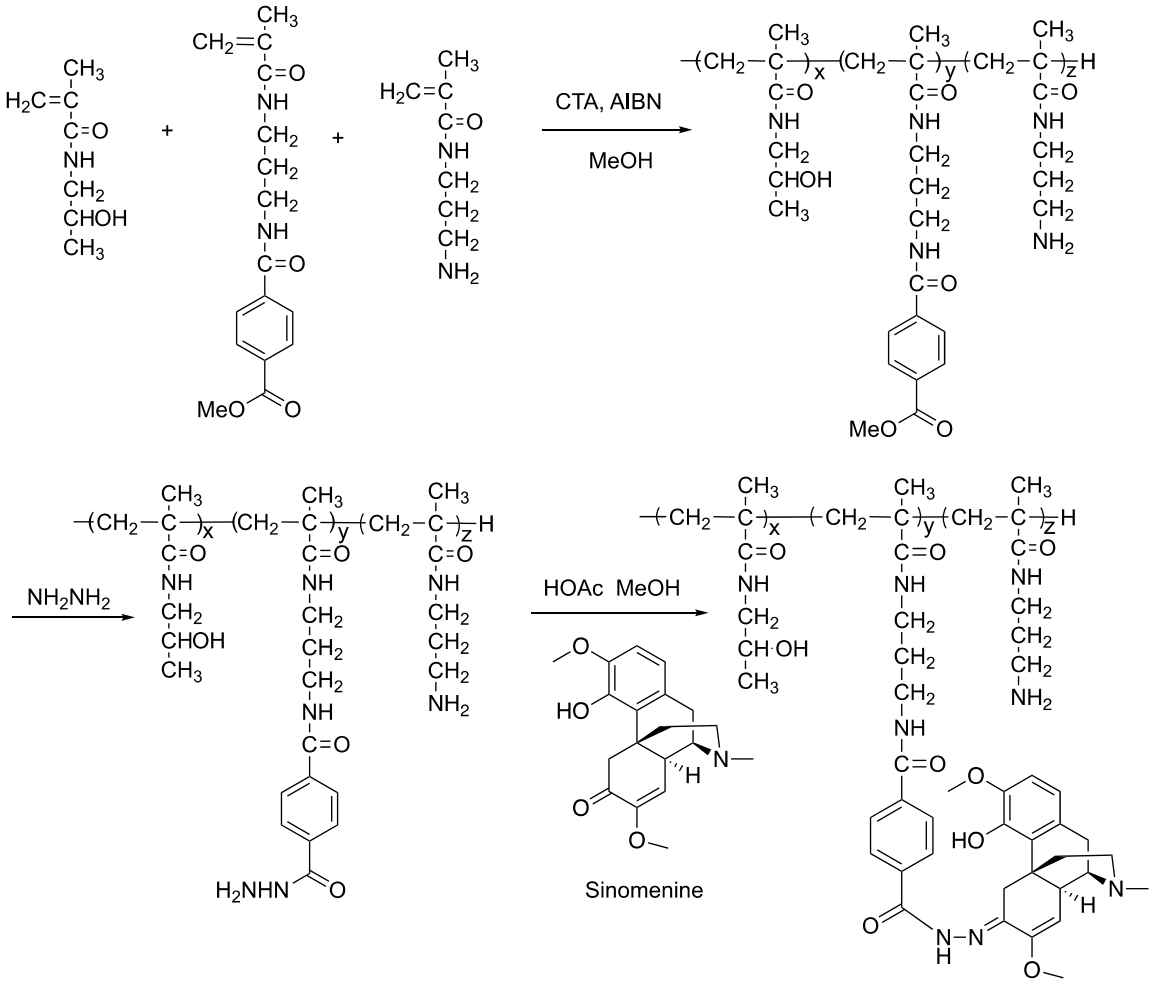

Figure 2.1 Synthesis route of ProGel Sinomenine. CTA, chain transfer agent; AIBN, 2,2′-azobisisobutyronitrile; MeOH, methanol; NH_2NH_2, hydrazine monohydrate; HOAc, acetic acid.

2.2.4 Synthesis of IRDye800CW labeled ProGel Sinomenine

In order to label with IRDye800, ProGel Sinomenine (40 mg), IRDye 800 NHS ester (0.8 mg) and triethylamine (4 mg) were dissolved in dimethylformamide (DMF) (1 mL). This solution was stirred overnight at room temperature and kept in the dark. The resultant solution was separated by column chromatography (LH-20) to get the final product of 38 mg of IRDye-labeled ProGel Sinomenine.

2.2.5 Synthesis of Alexa Flour 647 labeled ProGel Sinomenine

To synthesize Alexa Flour 647 labeled ProGel Sinomenine, Alexa 647 NHS ester (0.8mg), ProGel Sinomenine (40 mg), and triethylamine (4mg) were dissolved in DMF (1 mL). The resultant solution was stirred overnight at room temperature and kept in the dark. The solution was purified by column chromatography (LH-20) to earn a product of 39 mg of Alexa Flour 647 labeled ProGel Sinomenine.

2.2.6 Characterization of ProGel Sinomenine

The synthesized ProGel Sinomenine was characterized for its drug content and molecular weight. The dispersity and both the weight average molecular weight (Mw) and the number average molecular weight (Mn) of the synthesized copolymer was determined by size exclusion chromatography using the ÄKTA FPLC system equipped with UV and RI detectors. Hydrolysis method was adopted to quantitate the content of sinomenine in ProGel Sinomenine. The copolymer (1 mg/mL) was hydrolyzed overnight in 0.1N HCl by placing in a variable speed tube rotator. The next day, the solution was neutralized using 0.1N sodium hydroxide (NaOH) and evaluated on the HPLC system. The parameters set on the system to perform the analysis are: mobile phase, methanol (0.1% triethylamine): water (70:30); injection volume, 10µL; UV detection, 265 nm; flow rate, 0.5 mL/min; temperature, 30°C. The study was performed in triplicates.

2.2.7 Preliminary *in vitro* hydrogel release study of ProGel Sinomenine

To evaluate the release of sinomenine from the ProGel sinomenine, a membrane less dissolution method was used. The hydrogel was formed in a syringe (1 mL) at room temperature (~22°) and added to the glass vials containing 5 mL of various buffer solutions. The buffer solutions used to determine the release behavior are acetate buffer (0.1 M, pH 5.0 and pH 6.5) and phosphate buffer (0.1M, pH 7.4). These vials were kept in a water bath set at 37°C and were subjected to gentle agitation constantly. The releasing solution (1 mL) was withdrawn from all the vials at predetermined time points, neutralized with NaOH as appropriate and stored at -80°C to be analyzed by HPLC.

2.2.8 Sol-gel phase transition diagram for ProGel Sinomenine

The phase transition diagram for ProGel Sinomenine was established by performing a simple test tube inversion method. The various concentrations of ProGel Sinomenine (25 and 30% w/v) were prepared in an eppendorf tube by dissolving the drug in cold distilled water and complete dissolution was ensured. A hot plate was used to achieve the desired temperatures for the diagram. At specific temperature, the tubes were inverted to check the fluidity of the polymeric solution. It was considered as gel when the solution visually showed no fluid behavior. The temperature range for evaluation was from 10-40°C with a temperature increase of 1°C between each temperature.

2.2.9 Statistical analysis

Data are shown as mean ± SD. One-way analysis of variance (ANOVA) was used to analyze the data on GraphPad prism 8.03 (GraphPad software, Inc.). The post hoc test for multiple comparison was done using Dunnett's T3 test.

2.3 Results

2.3.1 Characterization of ProGel Sinomenine

ProGel Sinomenine was synthesized by the mechanism of polymer analogous reaction. The number average molecular weight (M_n) and the weight average molecular weight of ProGel Sinomenine is around 8.54 KDa and 9.24 KDa respectively with a narrow dispersity index of 1.081. To determine the amount of sinomenine loaded in ProGel Sinomenine, hydrolysis method followed by HPLC was taken up. The drug loading was around 20.4 wt%.

2.3.2 Preliminary *in vitro* hydrogel release study of ProGel Sinomenine

The releasing behavior of sinomenine from ProGel Sinomenine was evaluated in conditions simulated as in living organisms. The various buffers used are acetate buffer (0.1 M, pH 5.0 and pH 6.5) and phosphate buffer (0.1M, pH 7.4). The use of pH 7.4 reflects the physiological condition, pH 6.5 is the pH commonly found in the inflamed tissue, and pH 5.5 resembles the pH present in the lysosomal compartment of the cells where the drug is comparatively released more. As we can see from figure 2.2 there is very slow release at pH 6.5 and 7.4 and a more rapid release at pH 5. At around 170 hours, there is a release ~20% at pH 5.

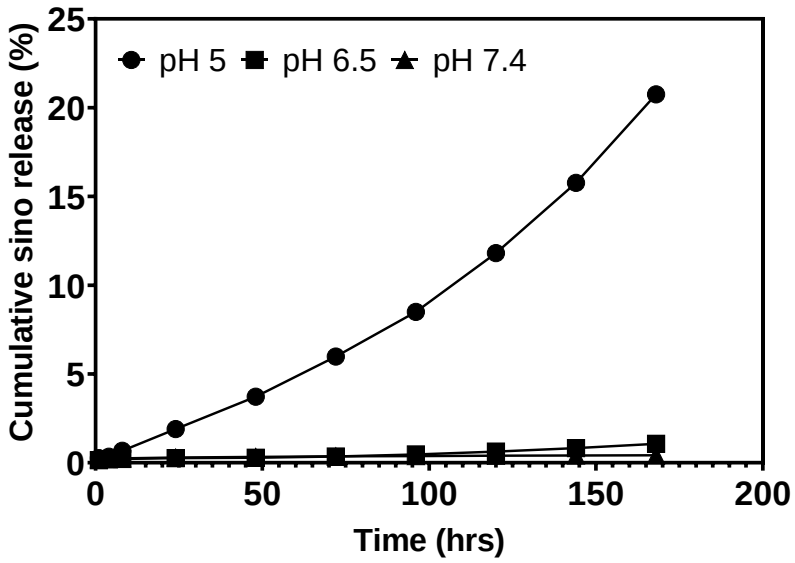

Figure 2.2 The preliminary in vitro hydrogel release of sinomenine in different pH buffers.

2.3.3 Sol-gel Phase transition diagram for ProGel Sinomenine

The test tube inversion method was used to create the phase transition diagram for ProGel Sino. A homogenous polymeric solution of concentrations 25 and 30 % w/v were prepared. From the diagram (Figure 2.4), we can identify the three regions of sol, gel, and syneresis. The gelation temperature (T_{gel}) for both the concentrations was 16 °C. This gel like behavior was confirmed when the polymeric solution showed no fluidity. The syneresis temperature for 25 and 30 % w/v was 22 and 24 °C, respectively. The thermoresponsive behavior of ProGel Sino can be seen from the pictorial representation below.

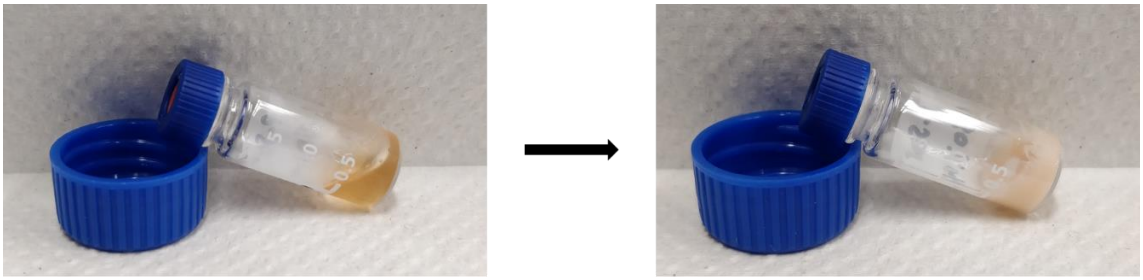

4 °C 22 °C

Figure 2.3 Picture of ProGel sinomenine in the injectable form at 4 °C and in the gel form at 22 °C (30 % w/v).

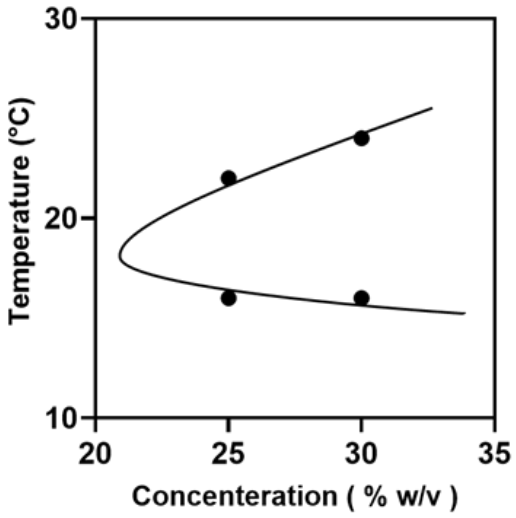

Figure 2.4 The sol-gel phase transition diagram for ProGel sinomenine. The diagram shows the gelation temperature (T_{gel}) and syneresis temperature for the concentrations 25 and 30 % (w/v).

2.4 Conclusion

In this study, we synthesized a HPMA copolymer conjugate of sinomenine which portrayed thermoresponsive behavior leading to the formation of hydrogel at elevated temperature. The chemically conjugated sinomenine to HPMA by an acid liable linker resulted in the release of sinomenine at low pH which is found at the inflamed site. Therefore, we successfully synthesized and characterized the macromolecular prodrug.

CHAPTER 3

IN VIVO THERAPEUTIC EFFICACY OF PROGEL SINOMENINE IN MONOARTICULAR ANTIGEN INDUCED ARTHRITIS (MAA) MODEL

3.1 Introduction

Sinomenine is known to be effective against rheumatic diseases but like any other drug they come with some limitations. Hence, various research groups focused on developing novel delivery systems and alternative routes of administration to overcome the limitations as mentioned in the previous chapters. The use of in situ forming hydrogel especially administering it via intra-articular injections will help in maintaining high concentrations of the drug at the injected site and also prevent the systemic toxicity sinomenine causes. In the previous chapter we synthesized a macromolecular prodrug of sinomenine which was capable of forming hydrogel at elevated temperature. In this study, we evaluated the therapeutic and analgesic efficacy of ProGel Sinomenine administered by intra-articular injection in an animal model of monoarticular antigen induced arthritis (MAA). Various behavioral methods with and without stimulus were adopted to analyze the pain tolerance in the animals to assess the analgesic efficacy of ProGel Sinomenine.

3.2 Materials and methods

3.2.1 Materials

Dulbecco's modified eagle medium (DMEM), trypsin-EDTA and penicillin-streptomycin were purchased from Gibco (Grand Island, NY, USA). Macrophage Raw 264.7 cells were formerly purchased from ATCC (Manassas, VA, USA). Fetal bovine serum (FBS) was purchased from Gemini BenchMark (West Sacramento, CA, USA). 3-(4,5-dimethyl-thiazol-2yl)-2,5-diphenyltetrazoliumbromide (MTT) and methyl bovine

serum albumin was bought from Sigma-Aldrich (Saint Louis, MO, USA). Heat killed Mycobacterium tuberculosis strain H37RA was obtained from Fisher Scientific (Pittsburgh, PA, USA). The reagent rotors were obtained from Zoetis, USA. All other solvents and reagents if not mentioned were purchased from either Sigma-Aldrich (Saint Louis, MO, USA) or Fisher Scientific (Pittsburgh, PA, USA).

3.2.2. Instruments

The static weight bearing test was performed using the incapacitance tester (Columbus Instruments, Columbus, OH). The pressure application measurement (PAM) test was evaluated using the Ugo Basile PAM unit (Ugo Basil 21025 Comerio, Varese, Italy) and the tail flick latencies using the Ugo Basile Talk Flick Unit (Ugo Basile SRL. Varese, Italy). Xenogen IVIS® Spectrum live animal imaging system (PerkinElmer Inc., Waltham, MA, USA) was used to perform the biodistribution study on the animals. To check the progress of decalcification of the bones, the X-ray system from Faxitron® MX-20 system (Faxitron Bioptics, LLC, Tucson, AZ) was used. The animal tissues were embedded in paraffin using the Kedee embedding instrument (Jinhua city, China). And the paraffin embedded tissues were sectioned using the Leica RM2255 microtome (Leica Biosystems, Buffalo Grove, IL). The chemistry and hematology levels of the animals were analyzed using the Vetscan® VS2 chemistry analyzer and Vetscan® HM5 hematology analyzer, respectively.

3.2.3 Induction of monoarticular antigen induced arthritis (MAA) model

The Lewis rats (male, 175-200 g) were procured from Charles River Laboratories. Upon arrival, they were acclimatized for one week with ad libitum access to food pellets and water. The rats received two subcutaneous injections, one week apart, of complete Freund's adjuvant comprising of methyl bovine serum albumin (mBSA, 2mg/mL) and heat killed *Mycobacterium tuberculosis* strain H37RA (2mg/mL) in distilled water and paraffin

oil, respectively. Two weeks after the second subcutaneous injection the animals received a booster injection of mBSA. This booster shot was administered intra-articularly (500 µg in 50µl of distilled water) to the left knee joint capsule of the rats. The establishment of monoarticular arthritis in the left knee joint was proved by the swelling of the joint and poor bearing. All the animal experiments were performed in complete conformity with the protocol as approved by the Institutional Animal Care and Use Committee (IACUC) of the University of Nebraska Medical Center.

3.2.4 Evaluation of therapeutic efficacy of ProGel Sinomenine in MAA rats

In order to analyze the analgesic and therapeutic benefits of ProGel Sinomenine, various pain evaluation tests were performed. These tests are commonly used as a measure of disease progression in the animal models of arthritis. The animals were randomly divided into 5 groups. The different groups are healthy control group (n=7), a saline control group (n=6), free Sinomenine group (20mg/kg) (n=6) and, ProGel Sinomenine (10 mg/kg and 20 mg/kg Sinomenine equivalent dose) (n=6 in both groups). The animals were treated by intra-articular injection on the inflamed left knee joint, the day after receiving the booster injection.

3.2.4.1 Weight bearing test

This test helps in measuring the weight distribution between the right and left hind legs of the animals. The distribution of weight between the hind legs can be used to indicate the level of discomfort caused due to the disease. An incapacitance tester was used to measure the weight distribution. The animals are placed in a chamber such that each of their hind legs are placed on a force transducer. These transducers can assess the body weight that the animals place on their hind legs. The paws were placed in the center of the force transducers and the body weight distribution (in grams) was estimated over a period of 3 seconds. All the data points are a mean of three, 3 second readings.

The resultant weight bearing score is shown as a ratio of the inflamed left limb in contrast to the sum of the weights on both the limbs resulting in a ratio of 50%. The weight bearing test was performed pre-induction, pre-treatment, and every day for 21 days post treatment.

3.2.4.2 Pressure Application Measurement (PAM)

This is a mechanical test used to measure the pain experienced on the knee joint of the rats by applying pressure. The PAM unit has a recording base with a digital display and a force transducer (maximum 1500-gram force) which is used to provide a steady pressure on the knee joints of the rat to measure their pain tolerance. The animal is held solidly, and the force transducer is placed on the medial side of the knee joint and a gradual force is applied. It is ensured that the increase in applied force across the joint is at the rate of 300 grams per second and the maximum time is five seconds. The end point of the test will be when the animal retreats their hind limbs or show any changes in their behavior like freezing of whisker or wriggling. The peak gram force (gf) at this end point will the recorded for analysis. This test is performed on both the hind limbs of the animals and was done pre-induction, pre-treatment and thrice a week post-treatment.

3.2.4.3 Tail flick test

The purpose of this test was to ensure that the analgesic effect produced by ProGel sinomenine does not have any off-course outcome in the spinal cord as provided by some opioids. It is an auxiliary test to prove the absence of the spinal cord analgesia. In order to perform this test, firstly the rats are restrained using a rat holder. Their tails were exposed to a focused beam of radiant heat at a point 3 cm from the tip of the tail. The tail flick latencies were determined as the interval between the outset of the heat stimulus and the spontaneous response of the tail to it. The animals not reacting within 15 seconds were removed from the instrument and were given the cut off latency of 15 seconds. These

latencies were measured pre-induction, pre-treatment, and everyday 7 days post-treatment.

3.2.4.4 Measurement of knee joint edema

The knee joints of both the hind limbs of the animal were measured using a digital vernier caliper. The joints were measured from the medial to the lateral side. They were evaluated pre-induction, pre-booster injection, pre-treatment, and everyday 21 days post-treatment.

3.2.5 *In-vivo* near-infrared biodistribution and retention study of ProGel Sinomenine in MAA rats

Two groups of animals, healthy group (n=5) and arthritis induced animals (n=5) were used to evaluate the biodistribution and retention of ProGel Sinomenine. After arthritis induction, the animals were administered with a mixture of IRDye800CW and Alexa fluor 647 labelled ProGel Sinomenine and ProGel Sinomenine (20mg/kg sinomenine equivalent) intra-articularly in the left knee joint and imaged using the IVIS imaging system. Before imaging, the fur from the hind legs of the animals were removed to forbid the attenuation of fluorescence signal and they were anesthetized with 2% isoflurane (with O_2) before and during imaging. They were imaged before treatment (baseline), 15 minutes, 2 hours, 8 hours, 1, 3, 5, 7, 14, and 21 days post-treatment. The parameters for capturing the images with respect to IRDye800CW are: Excitation- 778nm (filter: 745nm); Emission- 794 nm (filter: 800nm); Exposure time- auto; Field of view- 24.5 cm; Binning factor- 8; f number- 2. The acquired images were analyzed using the Living Image 4.5 software (PerkinElmer, Inc.). After 21 days post-treatment the vital organs and hind limbs of the animals were collected and imaged using Pearl Impulse small animal imaging system (LI-COR, Lincoln, NE, USA) for visualizing the fluorescence from the ex vivo organs. The images were acquired using the 800 nm and white light dual channel

procurement with a resolution of 85µm. The final images were adjusted to the same intensity scale with similar maximum and minimum values.

3.2.6 Safety and toxicity profiles of ProGel Sinomenine

To evaluate the effect of ProGel Sinomenine on liver and kidney functions, the blood from the animals were collected and analyzed on the Vetscan® VS2 chemistry analyzer and the hematology levels were evaluated using the Vetscan® HM5 hematology analyzer. Post 21 days treatment, the animals were subjected to an overdose of isoflurane and the blood was collected intracardially. The freshly collected blood was immediately transferred to a lithium heparin collection tube for the chemistry analysis and EDTA collection tube for hematology. The chemistry analysis was done using the rotor technology. These diagnostic profile rotors consist of reagents to give *in vitro* quantitative determinations of parameters like alanine aminotransferase (ALT), albumin (ALB), alkaline phosphate (ALP), amylase (AMY), creatinine (CRE), globulin (GLOB), total bilirubin, total protein, and electrolytes like phosphorous (PHOS), potassium (K^+), sodium (Na^+) etc. To analyze these, approximately 100µl of the blood sample was added to the rotor. And the hematology analyzer provided the complete blood count including the eosinophil and basophil levels.

3.2.7 Bone quality analysis using micro computed tomography

The hind limbs collected from the animals were preserved in buffered formalin. The quality of the bone in various treatment groups like free sinomenine and ProGel Sinomenine (low and high dose), the saline control group, and the healthy group were analyzed using the Skyscan 1172 micro computed tomography. All the samples were scanned with a voltage and current of 70 kV and 142 µA, respectively. The resolution of the camera was set at 13.1 µm. An aluminum filter (0.5 mm) was used to improve the exposure and quality of the image. The rotation step, frame averaging, and random

movement were set at 0.4 °, 6, and 10, respectively. Finally, they were all scanned with an angular rotation of 180 °. The obtained images were reconstructed using the NRecon software. To evaluate the morphometric parameters the trabecular bone at the proximal tibia was selected and the region of interest (ROI) was 60 slices from the growth plate and continued up to 99 slices. The bone morphometric parameters like percent bone volume (BV/TV), bone surface density (BS/TV), trabecular number (Tb.N), trabecular thickness (Tb.Th), and trabecular separation (Tb.Sp) were quantified using the CTVox software.

3.2.8 Histological analysis of the knee joint

After collecting the hind limbs and performing micro computed tomography on them, the left knee joints were trimmed from the limbs and excess tissues were removed from it. They were decalcified using 5% formic acid to perform the histological studies. The elimination of calcium from the tissues was made certain by using an X-ray system. The paraffin embedded tissues were sectioned at 8 µm using a microtome. The tissue sections were then checked for synovial cell lining hyperplasia, pannus formation, mononuclear cell infiltration, cellular infiltration in the cartilage, and bone erosion using Hematoxylin and eosin (H&E) staining.

3.2.9 Cell viability study

Raw 264.7 cells were cultured in the 96-well plate with a density of 1×10^4 cells per well overnight in an incubator with 5% CO2 and at 37 °C. On the following day, the culture medium was replaced with different concentrations of free sinomenine (10, 50, 100 µg/mL) and ProGel sinomenine (sinomenine equivalent concentrations (10, 50, 100 µg/mL)) and fresh growth media as control. The viability of cells was evaluated at 24 and 48 hours. MTT solution (10 µL) was then added to each well at the end of the treatment, that is, after 24 and 48 hours, followed by incubation at 37 °C for 4 hours. Lastly, the media

was removed from the wells and 100 µL of DMSO was added to each well to solubilize the formazan. The absorption was recorded using a microplate reader at 570 nm.

3.2.10 Statistical analysis

Data are shown as mean ± SD. One-way analysis of variance (ANOVA) was used to analyze the data on GraphPad prism 8.03 (GraphPad software, Inc.). The post hoc test for multiple comparison was done using Dunnett's T3 test. For the pain evaluation studies, two-way analysis of variance (ANOVA) was used and the post hoc test for multiple comparison was done with Tukey's test.

3.3 Results

3.3.1 Weight bearing test

The weight bearing scores for all the treatment groups was calculated as (weight on left leg/ (weight on right leg+ weight on left leg)) *100. There was a significant difference in the score between the saline and P-Sino high dose group from day 2 post-treatment. The P-Sino high group showed an improvement in the score from day 7 post-treatment and there was no statistical difference between the healthy and P-Sino high group on day 11 and 15 post-treatment. This shows that P-Sino high group had a better analgesic effect compared to the free Sino and P-Sino low group. But from day 16 post-treatment there was a statistical difference between the healthy and P-Sino high group indicating a possible drop in the analgesic effect (Figure 3.1). This effect could be due to the slow releasing behavior of the drug (Fig 2.2).

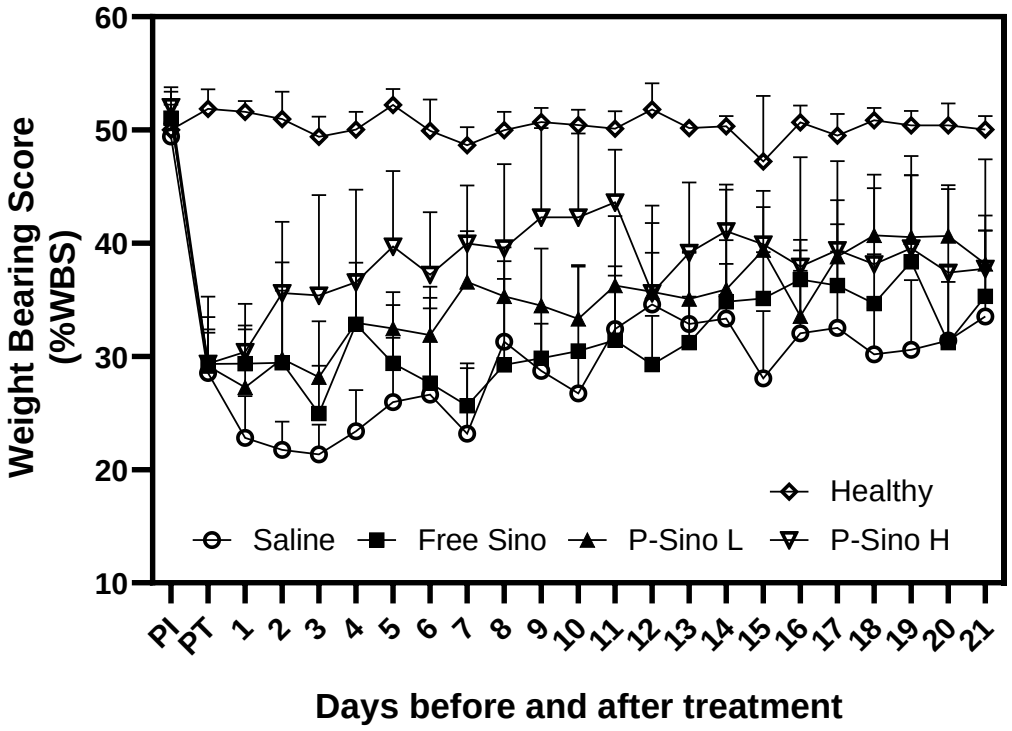

Figure 3.1 The percent Weight Bearing Score (%WBS) for MAA and healthy rats. PI, Pre-induction; PT, Pre-treatment; P-Sino L, ProGel Sinomenine low dose group; P-Sino H, ProGel Sinomenine high dose group.

Treatment groups	Pre-treatment	1D	2D	3D	4D	5D	6D	7D
Saline vs. Free sin	ns	ns	ns	ns	*	ns	ns	ns
Saline vs. P-sin low	ns	ns	ns	ns	*	ns	ns	****
Saline vs. P-sin high	ns	ns	****	****	***	****	**	****
Saline vs. Healthy	****	****	****	****	****	****	****	****
Free sin vs. P-sin low	ns	ns	ns	ns	ns	ns	ns	**
Free sin vs. P-sin high	ns	ns	ns	**	ns	**	*	****
Free sin vs. Healthy	****	****	****	****	****	****	****	****
P-sin low vs. P-sin high	ns	ns	ns	ns	ns	ns	ns	ns
P-sin low vs. Healthy	****	****	****	****	****	****	****	***
P-sin high vs. Healthy	****	****	****	****	****	***	****	*

Treatment groups	8D	9D	10D	11D	12D	13D	14D	15D
Saline vs. Free sin	ns	ns	ns	ns	ns	ns	ns	ns
Saline vs. P-sin low	ns	ns	ns	ns	ns	ns	ns	**
Saline vs. P-sin high	*	****	****	**	ns	ns	ns	***
Saline vs. Healthy	****	****	****	****	****	****	****	****
Free sin vs. P-sin low	ns	ns	ns	ns	ns	ns	ns	ns
Free sin vs. P-sin high	**	***	***	***	ns	ns	ns	ns
Free sin vs. Healthy	****	****	****	****	****	****	****	***
P-sin low vs. P-sin high	ns	ns	*	ns	ns	ns	ns	ns
P-sin low vs. Healthy	****	****	****	****	****	****	****	*
P-sin high vs. Healthy	**	*	*	ns	****	**	*	ns

Treatment groups	16D	17D	18D	19D	20D	21D
Saline vs. Free sin	ns	ns	ns	ns	ns	ns
Saline vs. P-sin low	ns	ns	**	**	*	ns
Saline vs. P-sin high	ns	ns	ns	*	ns	ns
Saline vs. Healthy	****	****	****	****	****	****
Free sin vs. P-sin low	ns	ns	ns	ns	*	ns
Free sin vs. P-sin high	ns	ns	ns	ns	ns	ns
Free sin vs. Healthy	****	****	****	***	****	****
P-sin low vs. P-sin high	ns	ns	ns	ns	ns	ns
P-sin low vs. Healthy	****	**	**	**	**	***
P-sin high vs. Healthy	****	**	****	**	****	***

Table 3.1 The statistical significance data for the percent Weight bearing score (%WBS) for the different treatment groups over the time course measured. Two-way analysis of variance (ANOVA), followed by the post hoc test for multiple comparison with Tukey's test. *, P≤0.05; **, P≤0.01; ***, P≤0.001; ****P≤0.0001.

3.3.2 Pressure Application Measurement (PAM)

The data from the pressure application test was expressed as a ratio of the peak gram force (gf) in arthritis induced left hind leg by the right hind leg. There was a significant different between the saline and the healthy group from before the treatment until the 16th day post treatment. A significant difference between free Sino and P-Sino high group was seen only on day 13. Like the weight bearing test, the PAM score showed an improvement from day 7 post-treatment with no statistical significance between the P-Sino high and healthy group. This shows that the animals experiences local analgesic effect from the 7th day post-treatment.

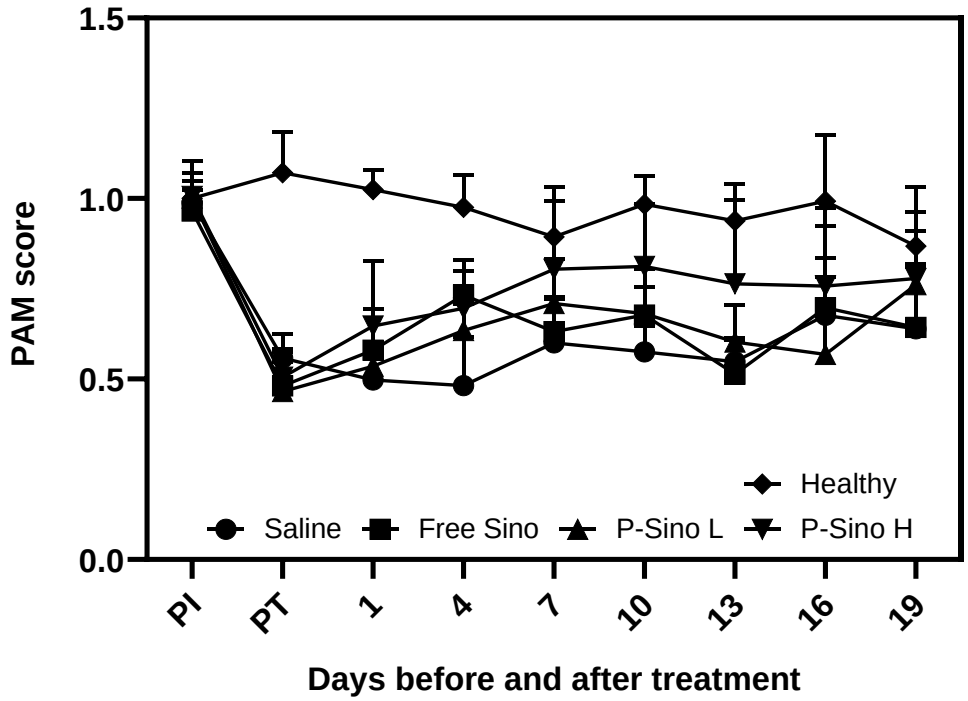

Figure 3.2 The PAM score for the MAA and healthy rats. PI, Pre-induction; PT, Pre-treatment; P-Sino L, ProGel Sinomenine low dose; P-Sino H, ProGel Sinomenine high

Treatment groups	Pre-treatment	1D	4D	7D	10D	13D	16D	19D
Saline vs. Free sin	ns	ns	*	ns	ns	ns	ns	ns
Saline vs. P-sin low	ns	ns	ns	ns	ns	ns	ns	ns
Saline vs. P-sin high	ns	ns	*	ns	*	*	ns	ns
Saline vs. Healthy	****	****	****	***	****	****	***	*
Free sin vs. P-sin low	ns	ns	ns	ns	ns	ns	ns	ns
Free sin vs. P-sin high	ns	ns	ns	ns	ns	*	ns	ns
Free sin vs. Healthy	****	****	**	**	***	****	***	*
P-sin low vs. P-sin high	ns	ns	ns	ns	ns	ns	ns	ns
P-sin low vs. Healthy	****	****	****	ns	***	****	****	ns
P-sin high vs. Healthy	****	****	**	ns	ns	ns	*	ns

dose Table 3.2 The statistical significance data for Pressure Application Measurement (PAM) for the different treatment groups over the time course measured. Two-way analysis of variance (ANOVA), followed by the post hoc test for multiple comparison with Tukey's test. *, P≤0.05; **, P≤0.01; ***, P≤0.001; ****P≤0.0001.

3.3.3 Tail flick test

The tail flick latencies (sec) obtained from the test were shown as the percent of maximum possible effect (% MPE). The %MPE was calculated as $((L_1-L_0)/(15-L_0))$ *100 where L_1 is the post-drug latency, L_0 is the pre-drug latency. The animals which did not react within 15 seconds, a latency of 15 seconds was designated to them. There was no statistical significance between any of the groups except on the days as shown in figure 3.3. This auxiliary test shows that P-Sino has no spinal cord analgesia.

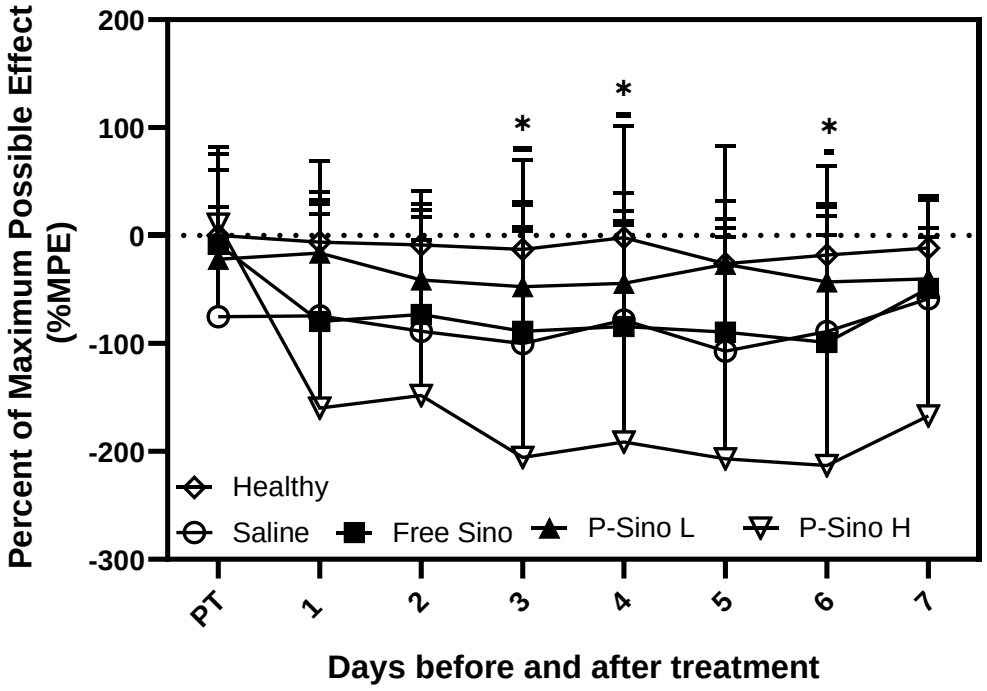

Figure 3.3 The tail flick latency values for the MAA and healthy rats. PT, Pre-treatment. P-Sino L, ProGel Sinomenine low dose group; P-Sino H, ProGel Sinomenine high dose group. *, P≤0.05.

3.3.4 Measurement of Knee joint edema

The swelling of the knee joint was measured from the medial to the lateral side using a digital caliper. As we can see from figure 3.4, there is a statistical difference between the healthy and P-Sino high group from the day after the treatment until the end of the study. Though there was a drop in statistical significance (table 3.3) between these groups on some days, the joint swelling did not reduce to the level of healthy animals. A statistical difference between free Sino and P-Sino high group was seen only on day 15 post-treatment and no statistical difference between saline and P-Sino high group.

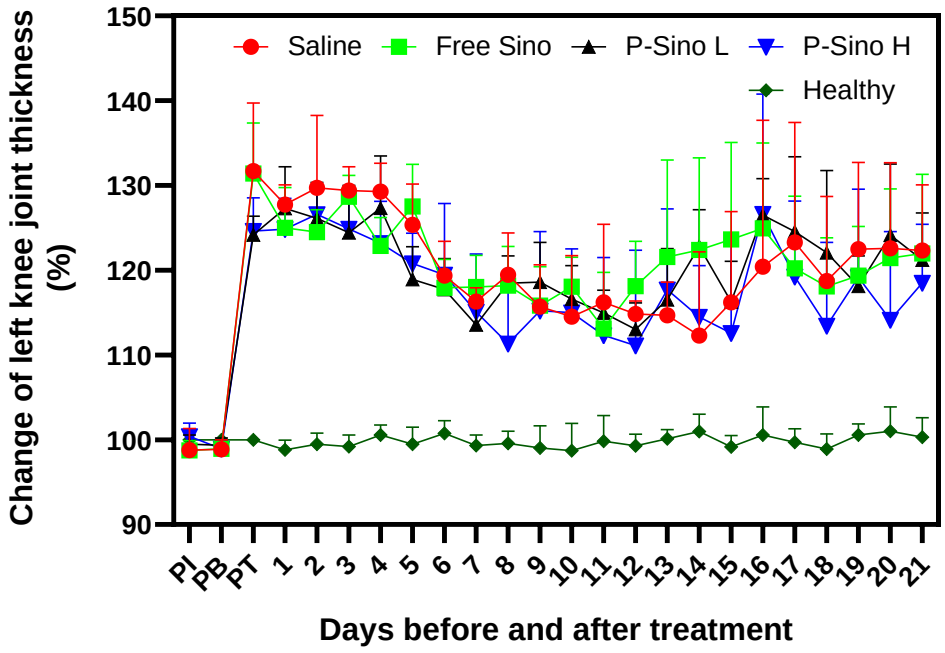

Figure 3.4 The change in left knee joint thickness of MAA and healthy rats. PI, Pre-induction; PB- Pre-booster; PT, Pre-treatment; P-Sino L, ProGel Sinomenine low dose group; P-Sino H, ProGel Sinomenine high dose group.

Treatment groups	Pre-treatment	1D	2D	3D	4D	5D	6D	7D
Saline vs. Free sin	ns	ns	ns	ns	ns	ns	ns	ns
Saline vs. P-sin low	ns	ns	ns	ns	ns	ns	ns	ns
Saline vs. P-sin high	ns	ns	ns	ns	ns	ns	ns	ns
Saline vs. Healthy	****	****	****	****	****	****	****	****
Free sin vs. P-sin low	ns	ns	ns	ns	ns	ns	ns	ns
Free sin vs. P-sin high	ns	ns	ns	ns	ns	ns	ns	ns
Free sin vs. Healthy	****	****	****	****	****	****	****	****
P-sin low vs. P-sin high	ns	ns	ns	ns	ns	ns	ns	ns
P-sin low vs. Healthy	****	****	****	****	****	****	****	***
P-sin high vs. Healthy	****	****	****	****	****	****	****	****

Treatment groups	8D	9D	10D	11D	12D	13D	14D	15D
Saline vs. Free sin	ns	ns	ns	ns	ns	ns	*	ns
Saline vs. P-sin low	ns	ns	ns	ns	ns	ns	*	ns
Saline vs. P-sin high	ns	ns	ns	ns	ns	ns	ns	ns
Saline vs. Healthy	****	****	****	****	****	***	**	****
Free sin vs. P-sin low	ns	ns	ns	ns	ns	ns	ns	ns
Free sin vs. P-sin high	ns	ns	ns	ns	ns	ns	ns	*
Free sin vs. Healthy	****	****	****	**	****	****	****	****
P-sin low vs. P-sin high	ns	ns	ns	ns	ns	ns	ns	ns
P-sin low vs. Healthy	****	****	****	***	***	****	****	****
P-sin high vs. Healthy	**	****	****	**	**	****	***	***

Treatment groups	16D	17D	18D	19D	20D	21D
Saline vs. Free sin	ns	ns	ns	ns	ns	ns
Saline vs. P-sin low	ns	ns	ns	ns	ns	ns
Saline vs. P-sin high	ns	ns	ns	ns	ns	ns
Saline vs. Healthy	****	****	****	****	****	****
Free sin vs. P-sin low	ns	ns	ns	ns	ns	ns
Free sin vs. P-sin high	ns	ns	ns	ns	ns	ns
Free sin vs. Healthy	****	****	****	****	****	****
P-sin low vs. P-sin high	ns	ns	ns	ns	*	ns
P-sin low vs. Healthy	****	****	****	****	****	****
P-sin high vs. Healthy	****	****	***	****	**	****

Table 3.3 The statistical significance data for change in knee joint thickness for the different treatment groups over the time course measured. Two-way analysis of variance (ANOVA), followed by the post hoc test for multiple comparison with Tukey's test. *, P≤0.05; **, P≤0.01; ***, P≤0.001; ****P≤0.0001.

3.3.5 *In-vivo* near-infrared biodistribution and retention study of ProGel Sinomenine in MAA rats

A robust fluorescent signal was seen on the knee joint injected with ProGel Sino-IRDye800 labeled animals. The signals were observed in both the MAA and healthy rats as shown in figure 3.5. There was a sustained fluorescent intensity detected as soon as 15 mins until 21 days post-treatment. This shows the prolonged retention of ProGel Sino at the inflamed joint. The intensity of the signal is not evident from the image from the 7th day for both the groups due to normalizing the intensities to the same value for representation.

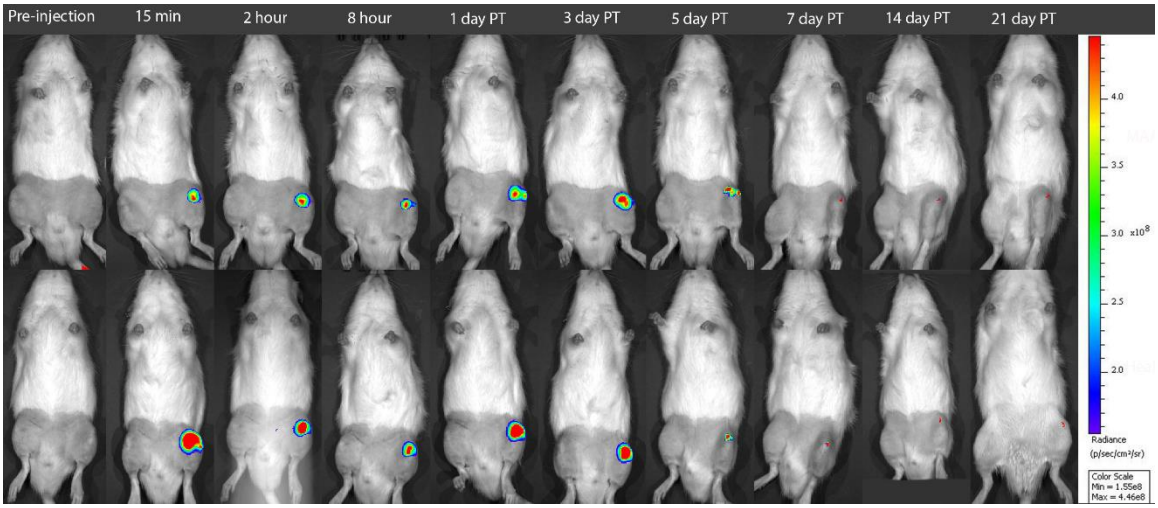

Figure 3.5 The representative images from the near-infrared biodistribution study showing the fluorescent signal at various time points post-injection. The top panel represents the same animal from the MAA group, and the bottom panel represent the animal from the healthy group. The intensity of the signal was adjusted to the same level for all the images. PT, Post-treatment.

3.3.6 Safety and toxicity profiles of ProGel Sinomenine

The hematologic profiles obtained showed some elevation in the levels of white blood cells (WBC) and lymphocytes in all the groups as expected. Though a statistical difference was seen in the levels of these cells between the P-Sino high and healthy group they were within the range (as mentioned in the manufacturers (Vetscan HM5) manual). No difference in the levels of monocytes, neutrophils, and red blood cells (RBC) were observed between any of the groups. (Figure 3.6)

The levels of ALT, ALB, ALP, and AMY levels were significantly lower in all the groups compared to the healthy group. There was no significant difference seen in the levels of the various electrolytes analyzed (Figure 3.7). All the groups showed an increase in the content of total protein compared to the healthy group, but no statistical difference was seen between the P-Sino high and healthy group.

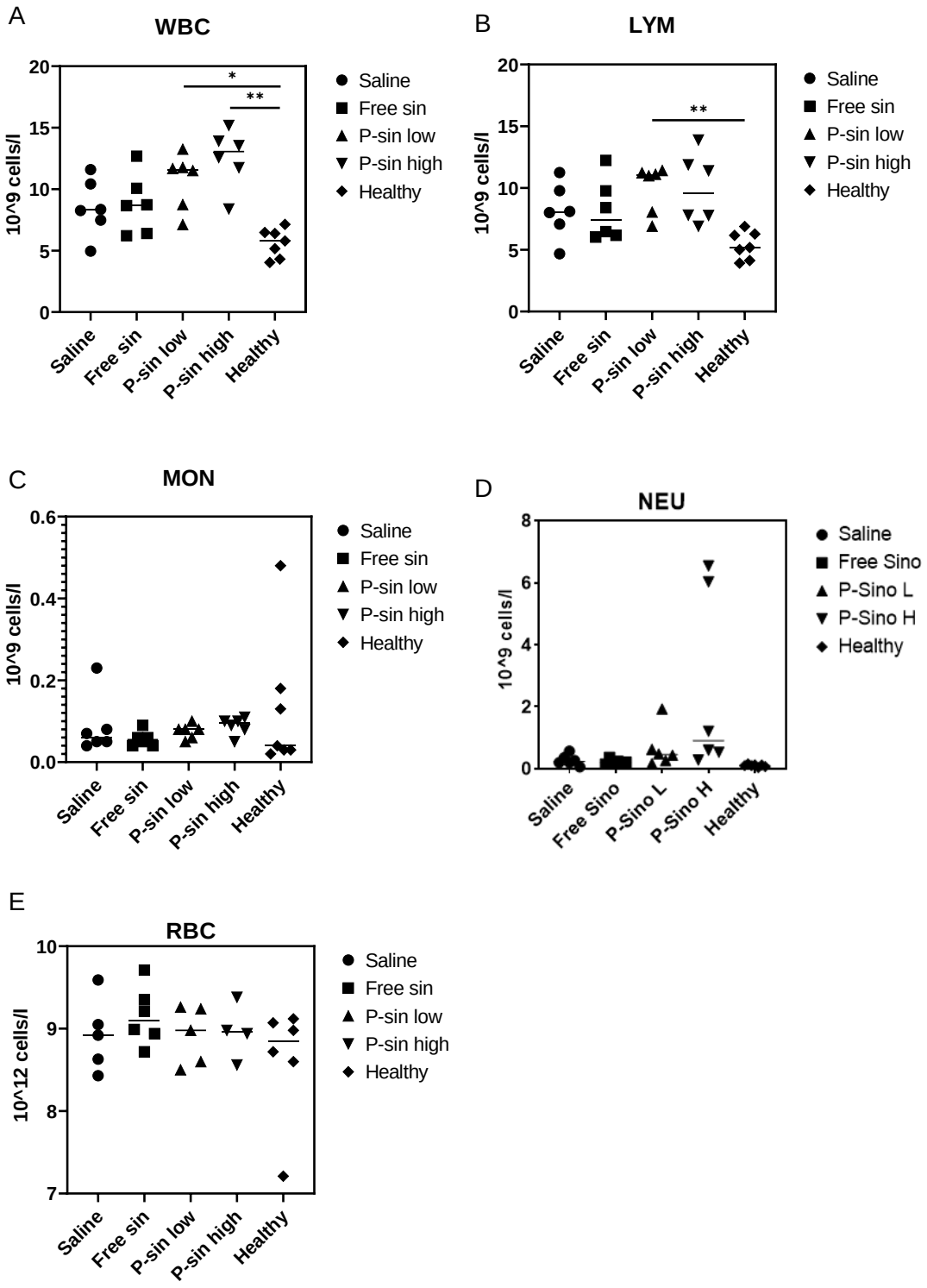

Figure 3.6 Hematologic profiles of various treatment groups. (A) White blood cells (WBC); (B) Lymphocytes; (C) Monocytes; (D) Neutrophils; (E) Red blood cells (RBC). *, P≤0.05; **P≤0.01.

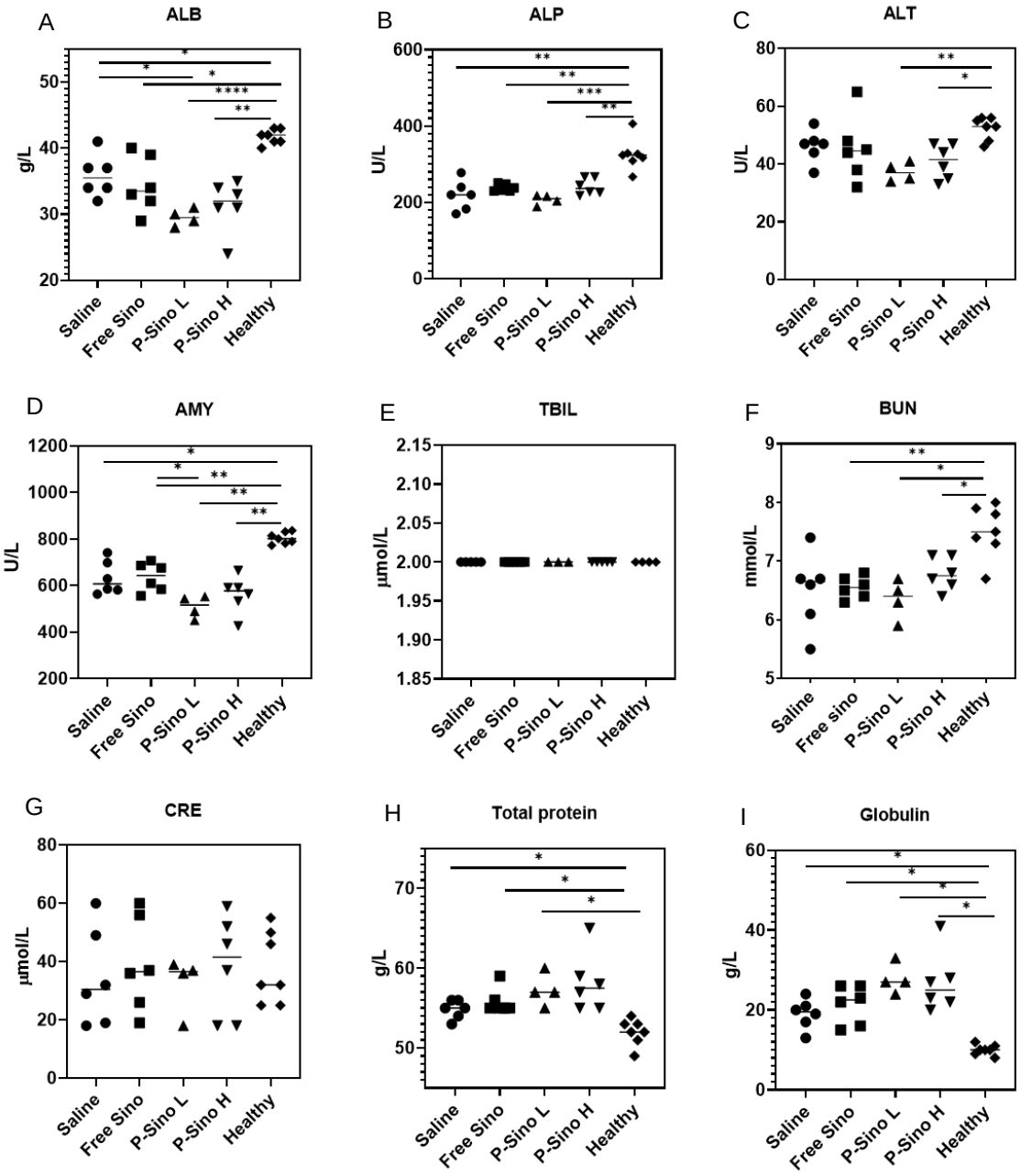
A
ALB
g/L
B
ALP
U/L
C
ALT
U/L
D
AMY
U/L
E
TBIL
μmol/L
F
BUN
mmol/L
G
CRE
μmol/L
H
Total protein
g/L
I
Globulin
g/L
Saline
Free Sino
P-Sino L
P-Sino H
Healthy

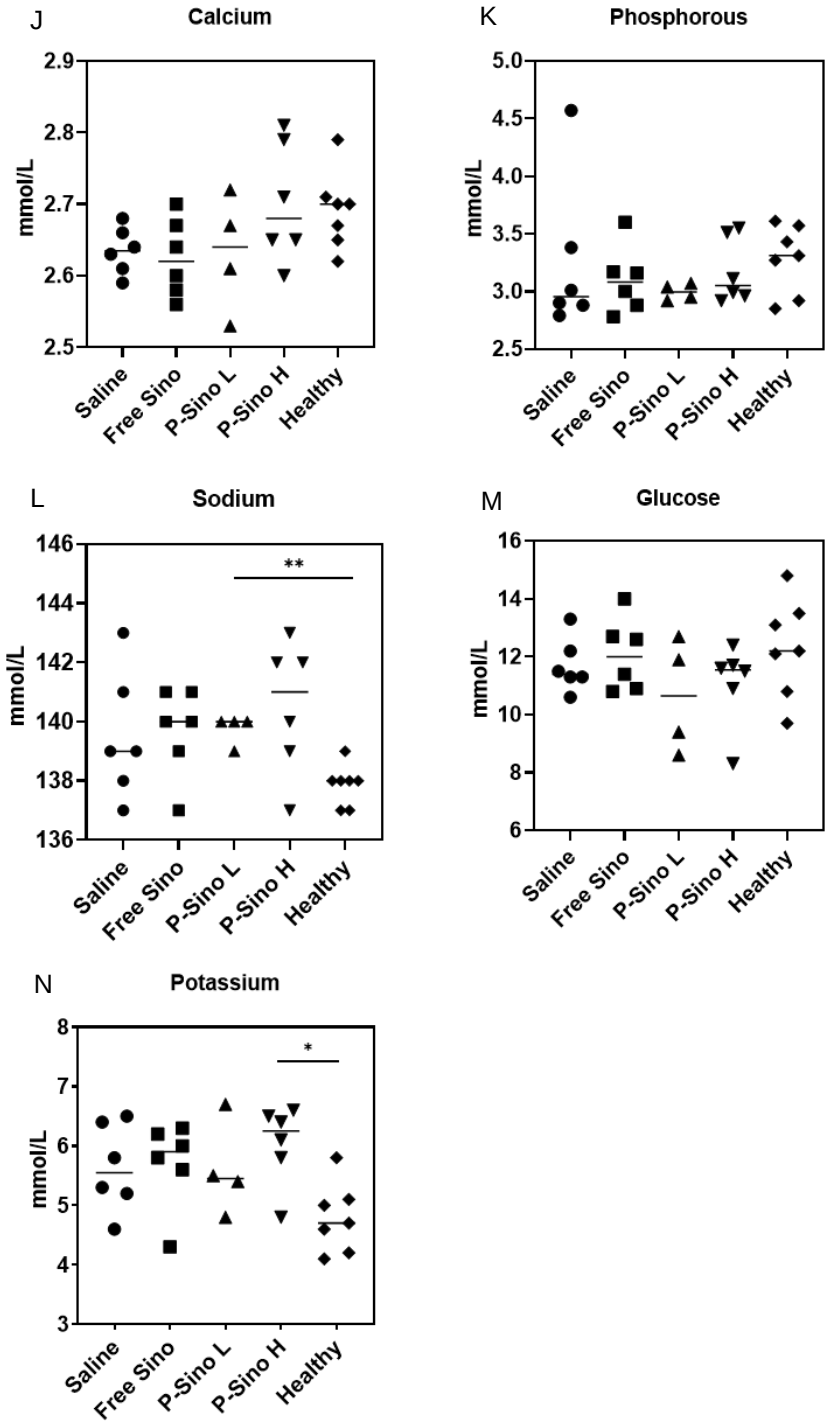

Figure 3.7 Blood chemistry profiles of the various treatment groups. (A) Albumin; (B)Alkaline phosphatase; (C) Alanine aminotransferase; (D) Amylase; (E) Total bilirubin; (F) Urea nitrogen; (G) Creatinine; (H) Total protein; (I) Globulin; (J) Calcium; (K) Phosphorous; (L) Sodium; (M) Glucose; (N) Potassium. *, P≤0.05; **, P≤0.01; ***, P≤0.001; ****, P≤0.0001.

3.3.7 Bone quality assessment using micro computed tomography

The extent of bone erosion and damage was evaluated in the left limb of all the five treatment groups. As seen from the representative 3D reconstructed image in figure 3.8, significant bone erosion and damage is seen in the femoral region of the limbs in the saline and the free Sino groups. Some amount of bone loss can also be identified in the trabecular region of the proximal tibia in the various treatment groups compared to the healthy group. This can be seen in the quantitative morphometric results such as the percent bone volume (BV/TV), bone surface density (BS/TV), trabecular thickness (Tb.Th), trabecular number (Tb.N), and trabecular separation (Tb.Sp). The percent bone volume is similar in the saline and the P-Sino high group and a much lower bone volume in the P-Sino low group. The bone surface density and trabecular number is significantly lower in the saline and P-Sino low group and showing a better density level in the P-Sino high group. The trabecular separation is similar in all the groups compared to the healthy group. And the trabecular thickness was significantly lower in the P-Sino low group compared to the healthy group and there was no significant difference in the other groups compared to the healthy group.

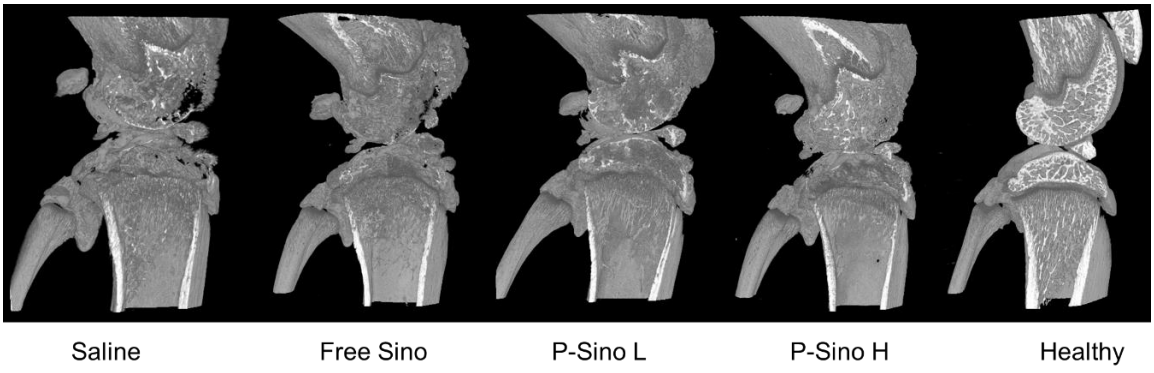

Figure 3.8 Representative 3D reconstructed micro-CT images (cross-sectional) of left knee joint of different treatment groups.

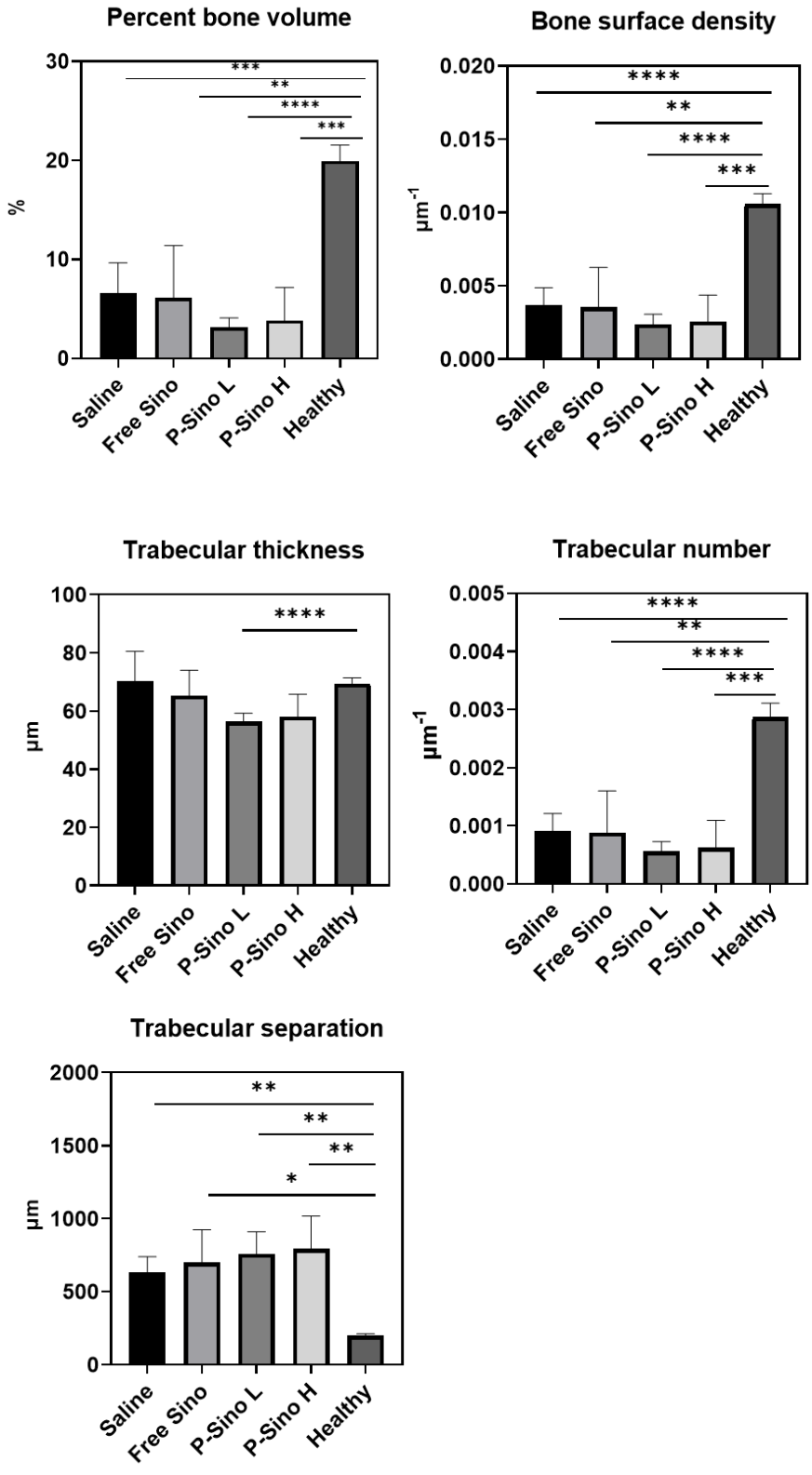

Figure 3.9 Morphometric parameters of the trabecular bone in the proximal tibia. *, P < 0.05; **, P ≤ 0.01; ***, P ≤ 0.001; ****, P ≤ 0.0001.

3.3.8 Cell viability study

The viability of Raw 264.7 macrophage cells were evaluated after the treatment with free sino and P-Sino at concentrations 10, 50, and 100 µg/mL. After 24 hours of treatment, we can observe an increase in the viability of cells in the P-Sino group and a decrease in the viability after 48 hours. As seen in some other experiments, the reduction in viability can be attributed to the delayed activation of the prodrug.

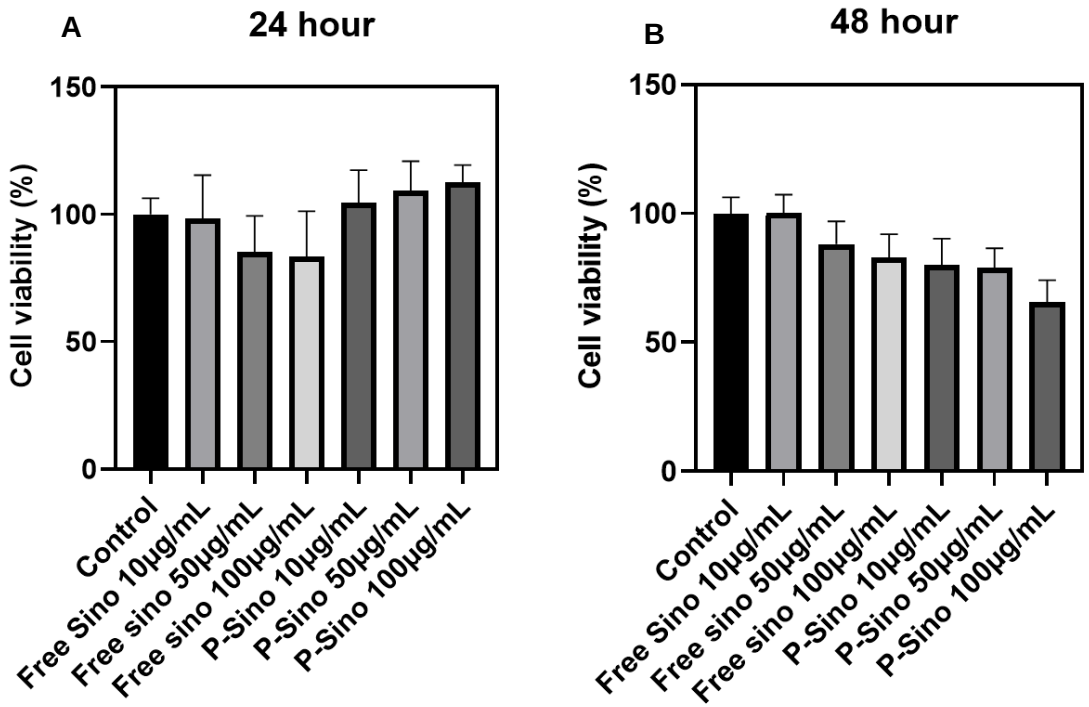

Figure 3.10 The cell viability evaluation of free sino and P-Sino groups in Raw 264.7 cells. A) Cell viability after 24 hours treatment. *, P ≤ 0.05 Control vs. P-Sino 100µg/mL, Free sino 50µg/mL vs. P-Sino 50µg/mL, and Free sino 100µg/mL vs. P-Sino 100µg/mL; **, P ≤ 0.01 Free sino 50µg/mL vs. P-Sino 100µg/mL. B) The Cell viability after 48 hours treatment. *, P ≤ 0.05 Control vs. Free sino 100µg/mL, Free Sino 10µg/mL vs. P-Sino 10µg/mL, and Free sino 100µg/mL vs. P-Sino 100µg/mL; **, P ≤ 0.01 Control vs. P-Sino 10µg/mL and Free sino 50µg/mL vs. P-Sino 100µg/mL; ***, P ≤ 0.001 Control vs. P-Sino 50µg/mL and Free Sino 10µg/mL vs. P-Sino 50µg/mL; ****, P ≤ 0.0001 Control vs. P-Sino 100µg/mL and Free Sino 10µg/mL vs. P-Sino 100µg/mL.

3.3.9 Histological analysis

The histological analysis was done to look into the micro-anatomy of the knee joint tissue. As we can see from the HE stained images of the left knee joint, the saline group has considerable bone erosion, infiltration of inflammatory cells, and synovial hyperplasia. Similarly even in the free sinomenine group, bone erosion and inflammatory cells were seen. But, the ProGel Sinomenine groups showed a slightly better result than the saline and free sino groups.

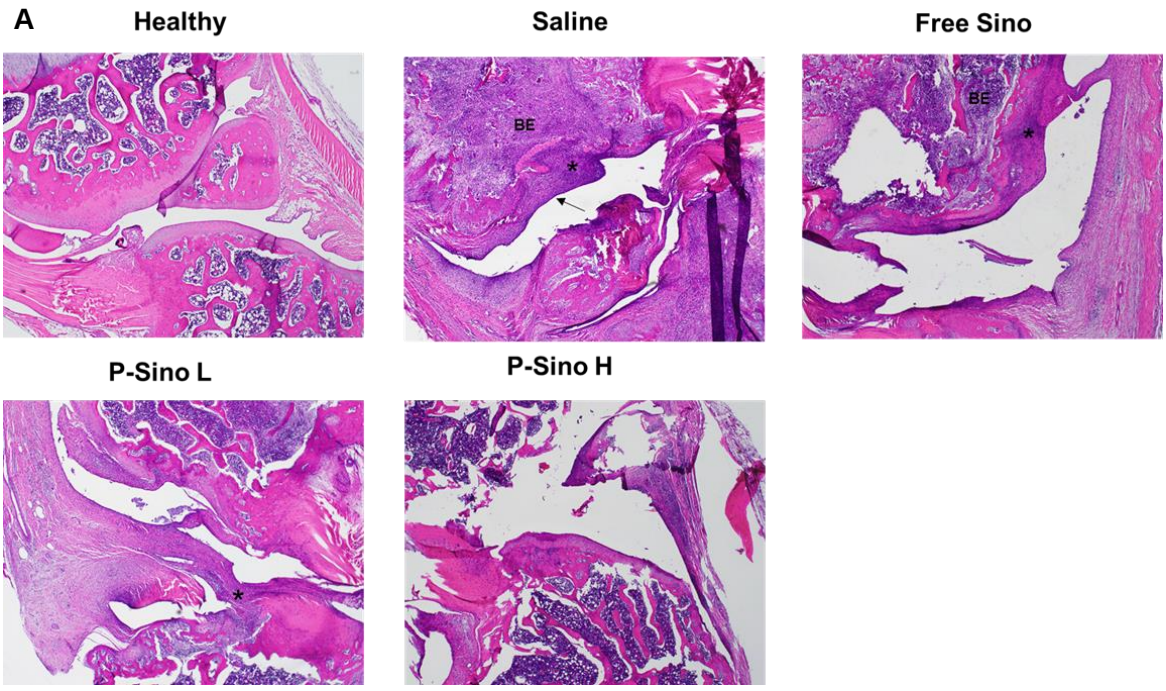

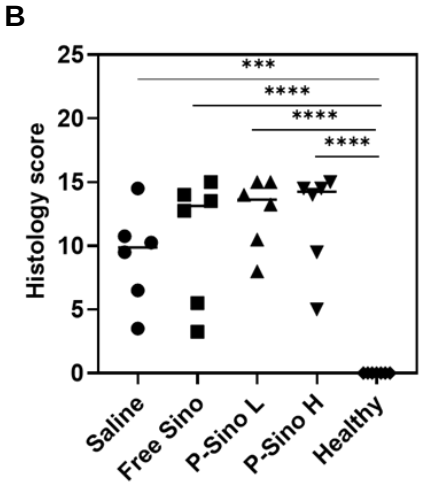

Figure 3.11 Histological analysis. A) Representative images after HE staining at 40X magnification and 500µm. BE indicates bone erosion; * respresents infiltration of inflammatory cells; black arrow indicates synovial hyperplasia. B) Histological scores of various treatment groups. ***, P ≤ 0.001; ****, P ≤ 0.0001.

3.4 Conclusion

In this chapter, we assessed the therapeutic and analgesic efficacy of ProGel Sinomenine by in intra-articular injection in a monoarticular antigen induced arthritis (MAA) model. The ProGel Sinomenine can form hydrogel and retain at the injected site for a period of twenty one days. We can also observe that ProGel Sinomenine has the ability to provide better local analgesic effect compared to the parent drug without any significant toxicity. Therefore, ProGel Sinomenine can be used as a potential drug for pain management in RA.

CHAPTER 4

SUMMARY

Rheumatoid arthritis is a chronic inflammatory disease that does not have a cure yet. The disease first manifests on smaller joints and then progresses to the bigger joints. The hallmark of the disease is inflammation of the synovial membrane and production of autoantibodies. The symptoms of RA are swelling of joints, stiffness, pain, and ultimately bone destruction. Though there are various classes of drugs available to reduce the symptoms of the disease, they have various side effects, and the management of pain still remains a concern. Often, they have short half-lives and poor bioavailability which leads to frequent dosing. In addition, biologics are extremely expensive and can result in a financial burden to the patients.

Due to the above-mentioned barriers, researchers are evaluating the effectiveness of alternatives like the traditional Chinese medicines (TCM). These natural extracts are available at a comparatively low cost and have a lower risk of side effects. TCM has been used to treat RA for more than 1000 years now. Recent studies have also shown the efficacy of TCM alone or in combination with western medicine against RA. They even have the capability of preserving the bone from destruction which was corroborated by the reduced levels of matrix metalloproteinase-3 (MMP-3). MMP-3 plays a vital role in the destruction of the cartilage and are related to the synovium, serving as a biomarker for bone damage [56-58].

Sinomenine is one such TCM that has been long used for the treatment of RA in China and Japan. It is a natural alkaloid which has numerous pharmacological effects ranging from anti-inflammatory, immunosuppression, analgesia, anti-angiogenesis, and anti-arthritic effects. Because of these they may be used as both NSAIDs and DMARD

[37]. But the long-term oral administration of sinomenine leads to gastrointestinal, cardiovascular, and liver toxicity etc. Since the concentration of sinomenine in the blood is varying the use of intra-articular injections will be advantageous in delivering high concentration of the drug at the desired site. This enables in overcoming the systemic toxicity and increasing the bioavailability of the drug. Administration of corticosteroids by IA is frequently seen in RA and OA. The U.S Food & Drug Administration (FDA) approved hyaluronic acid which is also popularly used in the treating OA. Yet again, the major drawbacks are the rapid clearance of the drug from the joint. Therefore, to have prolonged and constant drug availability the use of nanocarriers like hydrogels are instrumental [59]

Various research groups investigated the antinociceptive effects of sinomenine in inflammatory and neuropathic pain models and they showed the capability of sinomenine to produce an analgesic effect in these models [60-63]. In our current study, we assessed the analgesic and therapeutic efficacy of ProGel sinomenine administered by IA injection in a monoarticular antigen (MAA) induced arthritis model. The ProGel sinomenine was successfully synthesized by polymer analogous reaction with a drug loading of 20.4%. The thermoresponsive behavior of the drug can be seen in the phase transition diagram of ProGel sinomenine showing the sol and gel states with the gelation temperature of 16°C. This is corroborated by the image of the injectable and hydrogel form of the drug in figure 2.3. Further rheological characterization can be done to determine the viscoelastic behavior of the ProGel. Similarly, the *in vivo* biodistribution study shows the presence of the drug even after 21 days post-treatment. This implies the prolonged retention of the drug at the inflammatory site leading to sustained release and bioavailability of the drug.

From the results of the weight bearing study, a statistical difference in the weight bearing score is seen between the saline and ProGel Sino high dose group from day 2 post-treatment. And the ProGel Sino high dose group showed an improvement in the

score from day 7 post-treatment attributing to the analgesic effect. A possible delay in the analgesic effect could be due to the slow releasing behavior of the drug and time taken by the drug to become active at the inflamed site. Similarly, the pressure application test showed that ProGel Sino high group comparatively had a better local analgesic effect than free Sino and ProGel Sino low dose group. Also, there was no statistical significance in the PAM score between the high dose group and the healthy group animals from day 7 post-treatment. Therefore, from these results we can infer that ProGel Sino has the potential to elicit a local analgesic effect. To confirm that sinomenine does not produce any spinal cord analgesia, the tail flick test was performed. As shown in figure 3.3 the maximum possible effect (MPE) was around zero or below zero for the various treatment groups and there is no statistical difference in the MPE between any of the groups. This upholds that sinomenine has no spinal cord analgesia and they do not lead to the development of tolerance or addiction. On the contrary, there was no significant reduction in the swelling of the knee joint in the ProGel Sino or free Sino treatment groups. Literature evidences the anti-inflammatory effects of sinomenine in inflammatory models. Further dose escalation studies with higher doses are required to understand this better. The delayed release and activation of the prodrug could also be observed in the cell viability study performed. We can chemically modify the linker in the prodrug or add a hydrophobic counter ion to accelerate the activation of the prodrug and delay its dissolution.

To assess if ProGel sinomenine has any toxic effects, the blood chemistry profiles were checked. This profile helps in showing the kidney and liver functions and any possible effect the drug has on it. The albumin and liver enzyme levels were lower in all the groups compared to the healthy group. But there are evidences which show that sinomenine helps in improving the damage caused due to acute liver injury [64]. Therefore, we can conclude that ProGel Sino has no potential toxic or side effects.

Finally, ProGel sinomenine's capability in preserving the joint and bone quality was assessed by the micro-computed tomography. From the representative 3D reconstructed image, we can see a minor change in the structure the ProGel Sino groups compared to the saline group. But some of the morphometric parameters like the percent bone volume and trabecular separation was similar in the saline and ProGel Sino high group and for some parameters the ProGel Sino high group showed a better result. Literature shows the ability of sinomenine to protect the bone from destruction due to arthritis. But the sinomenine dose administered were ranging from 25 to 100 mg/kg with the 100 mg/kg dose showing the morphometric parameters being almost similar the control group[65]. Even in our study, the free Sino group showed closer results to the healthy group in regard to the significance level. A possible explanation of ProGel Sino being unable to elicit a similar result could be due to its relatively slow activation. Also, the narrow space in the knee joint restrained the dosing level. Further, the pharmacokinetics of the prodrug can be evaluated, and their versatility can be assessed in other inflammatory models like adjuvant induced polyarthritis model, OA model etc.

In this study, the therapeutic and analgesic efficacy of ProGel sinomenine in a monoarticular antigen induced arthritis model was successfully evaluated. The ability of ProGel Sino to form hydrogel at the inflamed site after the intra-articular injection and display an analgesic effect was validated. The retention and sustained release of the drug was corroborated thus fulfilling the need to improve the bioavailability of the drug. Ultimately, the toxic and safety profiles showcase the absence of any systemic toxicity. Therefore, with further studies ProGel Sinomenine can be used as a probable drug for the management of pain in RA.

Reference

1. Liang, H., et al., *Cationic nanoparticle as an inhibitor of cell-free DNA-induced inflammation.* Nat Commun, 2018. **9**(1): p. 4291.
2. Quan, L.D., et al., *The Development of Novel Therapies for Rheumatoid Arthritis.* Expert Opin Ther Pat, 2008. **18**(7): p. 723-738.
3. Zhou, H., et al., *Sinomenine ameliorates arthritis via MMPs, TIMPs, and cytokines in rats.* Biochem Biophys Res Commun, 2008. **376**(2): p. 352-7.
4. Cojocaru, M., et al., *Extra-articular Manifestations in Rheumatoid Arthritis.* Maedica (Bucur), 2010. **5**(4): p. 286-91.
5. Sager, Z.S., *Nurturing Medicine.* Jama, 2018. **320**(13): p. 1325.
6. Emery, P., et al., *Early referral recommendation for newly diagnosed rheumatoid arthritis: evidence based development of a clinical guide.* Ann Rheum Dis, 2002. **61**(4): p. 290-7.
7. Bullock, J., et al., *Rheumatoid Arthritis: A Brief Overview of the Treatment.* Med Princ Pract, 2018. **27**(6): p. 501-507.
8. Köhler, B.M., et al., *Current Therapeutic Options in the Treatment of Rheumatoid Arthritis.* J Clin Med, 2019. **8**(7).
9. Kurkó, J., et al., *Genetics of rheumatoid arthritis - a comprehensive review.* Clin Rev Allergy Immunol, 2013. **45**(2): p. 170-9.
10. Aho, K. and M. Heliövaara, *Risk factors for rheumatoid arthritis.* Ann Med, 2004. **36**(4): p. 242-51.
11. Oliver, J.E. and A.J. Silman, *Risk factors for the development of rheumatoid arthritis.* Scand J Rheumatol, 2006. **35**(3): p. 169-74.

12. Ong, C.K., et al., *An evidence-based update on nonsteroidal anti-inflammatory drugs.* Clin Med Res, 2007. **5**(1): p. 19-34.

13. Mamdani, M., et al., *Effect of selective cyclooxygenase 2 inhibitors and naproxen on short-term risk of acute myocardial infarction in the elderly.* Arch Intern Med, 2003. **163**(4): p. 481-6.

14. Liu, D., et al., *A practical guide to the monitoring and management of the complications of systemic corticosteroid therapy.* Allergy Asthma Clin Immunol, 2013. **9**(1): p. 30.

15. Benjamin, O., et al., *Disease Modifying Anti-Rheumatic Drugs (DMARD)*, in *StatPearls*. 2021, StatPearls Publishing Copyright © 2021, StatPearls Publishing LLC.: Treasure Island (FL).

16. Cronstein, B.N. and T.M. Aune, *Methotrexate and its mechanisms of action in inflammatory arthritis.* Nat Rev Rheumatol, 2020. **16**(3): p. 145-154.

17. Aletaha, D. and J.S. Smolen, *Diagnosis and Management of Rheumatoid Arthritis: A Review.* Jama, 2018. **320**(13): p. 1360-1372.

18. de La Forest Divonne, M., J.E. Gottenberg, and C. Salliot, *Safety of biologic DMARDs in RA patients in real life: A systematic literature review and meta-analyses of biologic registers.* Joint Bone Spine, 2017. **84**(2): p. 133-140.

19. Mody, G.M. and M.H. Cardiel, *Challenges in the management of rheumatoid arthritis in developing countries.* Best Pract Res Clin Rheumatol, 2008. **22**(4): p. 621-41.

20. Whittle, S.L., et al., *Multinational evidence-based recommendations for pain management by pharmacotherapy in inflammatory arthritis: integrating systematic literature research and expert opinion of a broad panel of rheumatologists in the 3e Initiative.* Rheumatology (Oxford), 2012. **51**(8): p. 1416-25.

21. Day, A.L. and J.R. Curtis, *Opioid use in rheumatoid arthritis: trends, efficacy, safety, and best practices.* Curr Opin Rheumatol, 2019. **31**(3): p. 264-270.

22. Richards, B.L., S.L. Whittle, and R. Buchbinder, *Antidepressants for pain management in rheumatoid arthritis.* Cochrane Database Syst Rev, 2011(11): p. Cd008920.

23. Richards, B.L., et al., *The efficacy and safety of antidepressants in inflammatory arthritis: a Cochrane systematic review.* J Rheumatol Suppl, 2012. **90**: p. 21-7.

24. Pirmardvand Chegini, S., J. Varshosaz, and S. Taymouri, *Recent approaches for targeted drug delivery in rheumatoid arthritis diagnosis and treatment.* Artif Cells Nanomed Biotechnol, 2018. **46**(sup2): p. 502-514.

25. Conigliaro, P., et al., *Challenges in the treatment of Rheumatoid Arthritis.* Autoimmun Rev, 2019. **18**(7): p. 706-713.

26. Xu, M., et al., *Sinomenine versus NSAIDs for the treatment of rheumatoid arthritis: a systematic review and meta-analysis.* Planta Med, 2008. **74**(12): p. 1423-9.

27. Liu, W., et al., *Effects and safety of Sinomenine in treatment of rheumatoid arthritis contrast to methotrexate: a systematic review and Meta-analysis.* J Tradit Chin Med, 2016. **36**(5): p. 564-77.

28. Sun, Y., Y. Yao, and C.Z. Ding, *A combination of sinomenine and methotrexate reduces joint damage of collagen induced arthritis in rats by modulating osteoclast-related cytokines.* Int Immunopharmacol, 2014. **18**(1): p. 135-41.

29. Zhou, Y.R., et al., *SND-117, a sinomenine bivalent alleviates type II collagen-induced arthritis in mice.* Int Immunopharmacol, 2015. **26**(2): p. 423-31.

30. Song, H., et al., *Enhanced transdermal permeability and drug deposition of rheumatoid arthritis via sinomenine hydrochloride-loaded antioxidant surface transethosome.* Int J Nanomedicine, 2019. **14**: p. 3177-3188.

31. Jiang, W., et al., *Analgesic Mechanism of Sinomenine against Chronic Pain.* Pain Res Manag, 2020. **2020**: p. 1876862.

32. Ng, J.P.L., et al., *The present and future synthetic strategies of structural modifications of sinomenine.* Organic Chemistry Frontiers, 2020. **7**(24): p. 4089-4107.

33. Li, X., et al., *Development of patch and spray formulations for enhancing topical delivery of sinomenine hydrochloride.* J Pharm Sci, 2010. **99**(4): p. 1790-9.

34. Liu, Z.Q., et al., *The pharmacokinetics and tissue distribution of sinomenine in rats and its protein binding ability in vitro.* Life Sci, 2005. **77**(25): p. 3197-209.

35. Zhang, M.F., et al., *Comparative pharmacokinetics study of sinomenine in rats after oral administration of sinomenine monomer and Sinomenium acutum extract.* Molecules, 2014. **19**(8): p. 12065-77.

36. Tsai, T.H. and J.W. Wu, *Regulation of hepatobiliary excretion of sinomenine by P-glycoprotein in Sprague-Dawley rats.* Life Sci, 2003. **72**(21): p. 2413-26.

37. Zhao, X.X., et al., *Sinomenium acutum: a review of chemistry, pharmacology, pharmacokinetics, and clinical use.* Pharm Biol, 2012. **50**(8): p. 1053-61.

38. Shu, Z., et al., *Polyvinylpyrrolidone microneedles for localized delivery of sinomenine hydrochloride: preparation, release behavior of in vitro & in vivo, and penetration mechanism.* Drug Deliv, 2020. **27**(1): p. 642-651.

39. Sun, Y., et al., *A novel enteric positioning osmotic pump capsule-based controlled release system of sinomenine hydrochloride: In vitro and in vivo evaluation.* Journal of Drug Delivery Science and Technology, 2019. **49**: p. 188-194.

40. Zhou, Y., et al., *Determination of sinomenine in cubosome nanoparticles by HPLC technique.* J Anal Methods Chem, 2015. **2015**: p. 931687.

41. Shen, Q., et al., *Sinomenine hydrochloride loaded thermosensitive liposomes combined with microwave hyperthermia for the treatment of rheumatoid arthritis.* Int J Pharm, 2020. **576**: p. 119001.

42. Chu, X., et al., *Characterization and In Vitro Permeation Study of Cubic Liquid Crystal Containing Sinomenine Hydrochloride.* AAPS PharmSciTech, 2018. **19**(5): p. 2237-2246.

43. Kopecek, J. and P. Kopecková, *HPMA copolymers: origins, early developments, present, and future.* Adv Drug Deliv Rev, 2010. **62**(2): p. 122-49.

44. Rautio, J., et al., *The expanding role of prodrugs in contemporary drug design and development.* Nat Rev Drug Discov, 2018. **17**(8): p. 559-587.

45. Vasey, P.A., et al., *Phase I clinical and pharmacokinetic study of PK1 [N-(2-hydroxypropyl)methacrylamide copolymer doxorubicin]: first member of a new class of chemotherapeutic agents-drug-polymer conjugates. Cancer Research Campaign Phase I/II Committee.* Clin Cancer Res, 1999. **5**(1): p. 83-94.

46. Quan, L.D., et al., *Development of a macromolecular prodrug for the treatment of inflammatory arthritis: mechanisms involved in arthrotropism and sustained therapeutic efficacy.* Arthritis Res Ther, 2010. **12**(5): p. R170.

47. Wang, D., et al., *Novel dexamethasone-HPMA copolymer conjugate and its potential application in treatment of rheumatoid arthritis.* Arthritis Res Ther, 2007. **9**(1): p. R2.

48. Jia, Z., et al., *Structural optimization of HPMA copolymer-based dexamethasone prodrug for improved treatment of inflammatory arthritis.* J Control Release, 2020. **324**: p. 560-573.

49. Weber, L., et al., *The Development of a Macromolecular Analgesic for Arthritic Pain.* Mol Pharm, 2019. **16**(3): p. 1234-1244.

50. Wei, X., et al., *Development of a Janus Kinase Inhibitor Prodrug for the Treatment of Rheumatoid Arthritis.* Mol Pharm, 2018. **15**(8): p. 3456-3467.

51. Hoare, T.R. and D.S. Kohane, *Hydrogels in drug delivery: Progress and challenges.* Polymer, 2008. **49**(8): p. 1993-2007.

52. Song, J., et al., *Preparation and evaluation of sinomenine hydrochloride in situ gel for uveitis treatment.* Int Immunopharmacol, 2013. **17**(1): p. 99-107.

53. Liu, J., et al., *Evaluation of pharmacokinetics and pharmaco-dynamics of sinomenine-hyaluronic acid conjugate after intra-articular administration for osteoarthritis treatment.* Drug Des Devel Ther, 2019. **13**: p. 657-665.

54. Liang, X., et al., *In situ hexagonal liquid crystal for intra-articular delivery of sinomenine hydrochloride.* Biomed Pharmacother, 2019. **117**: p. 108993.

55. Chytil, P., et al., *N-(2-Hydroxypropyl)methacrylamide-based polymer conjugates with pH-controlled activation of doxorubicin for cell-specific or passive tumour targeting. Synthesis by RAFT polymerisation and physicochemical characterisation.* Eur J Pharm Sci, 2010. **41**(3-4): p. 473-82.

56. Klimiuk, P.A., et al., *Serum matrix metalloproteinases and tissue inhibitors of metalloproteinases in different histological variants of rheumatoid synovitis.* Rheumatology (Oxford), 2002. **41**(1): p. 78-87.

57. Cai, X., et al., *The Bone-Protecting Efficiency of Chinese Medicines Compared With Western Medicines in Rheumatoid Arthritis: A Systematic Review and Meta-Analysis of Comparative Studies.* Front Pharmacol, 2018. **9**: p. 914.

58. Xia, X., et al., *Chinese Herbal Medicines for Rheumatoid Arthritis: Text-Mining the Classical Literature for Potentially Effective Natural Products.* Evid Based Complement Alternat Med, 2020. **2020**: p. 7531967.

59. Rai, M.F. and C.T. Pham, *Intra-articular drug delivery systems for joint diseases.* Curr Opin Pharmacol, 2018. **40**: p. 67-73.

60. Zhu, Q., et al., *Antinociceptive effects of sinomenine in a rat model of neuropathic pain.* Sci Rep, 2014. **4**: p. 7270.

61. Gao, T., et al., *Analgesic effect of sinomenine in rodents after inflammation and nerve injury.* Eur J Pharmacol, 2013. **721**(1-3): p. 5-11.

62. Wang, M.H., et al., *Activation of opioid mu-receptor by sinomenine in cell and mice.* Neurosci Lett, 2008. **443**(3): p. 209-12.

63. Lee, J.Y., et al., *Sinomenine produces peripheral analgesic effects via inhibition of voltage-gated sodium currents.* Neuroscience, 2017. **358**: p. 28-36.

64. Chen, H., et al., *Sinomenine Attenuates Acetaminophen-Induced Acute Liver Injury by Decreasing Oxidative Stress and Inflammatory Response via Regulating TGF-β/Smad Pathway in vitro and in vivo.* Drug Des Devel Ther, 2020. **14**: p. 2393-2403.

65. Liao, K., et al., *Sinomenine protects bone from destruction to ameliorate arthritis via activating p62(Thr269/Ser272)-Keap1-Nrf2 feedback loop.* Biomed Pharmacother, 2021. **135**: p. 111195.